ICARUS 94, 191–208 (1991)

Derivation of Midinfrared (5–25 μm) Optical Constants of Some Silicates and Palagonite

T. ROUSH[1]

San Francisco State University, Adjunct Professor, Department of Geosciences, 1600 Holloway Avenue, San Francisco, California 94132

J. POLLACK

NASA Ames Research Center, MS 245-3, Moffett Field, California 94035-1000

AND

J. ORENBERG

San Francisco State University, Department of Chemistry, 1600 Holloway Avenue, San Francisco, California 94132

Received January 18, 1991; revised August 7, 1991

The midinfrared 2000–400 cm^{-1} (5–25 μm) optical constants (real (n) and imaginary (k) indices of refraction) are presented for: (1) pyrophyllite; (2) kaolinite; (3) serpentine; (4) montmorillonite; (5) saponite; (6) palagonite; and (7) orthopyroxene. Comparison of the values derived here with those previously presented for serpentine, montmorillonite, and palagonite is generally quite good and discrepancies between values are probably due to either chemical differences between the actual samples or different techniques used to derive the values. For montmorillonite, saponite, and palagonite we were able to derive optical constants in the region of the H_2O-bending fundamental near 6 μm. We find that if a pellet of pure material can be produced with a mirror-like surface then the optical constants of clays and other noncohesive materials can be readily derived. © 1991 Academic Press, Inc.

1. INTRODUCTION

Recent reports concerning the midinfrared reflectance properties of silicates (Salisbury *et al.* 1987, Salisbury and Walter 1989, Walter and Salisbury 1989) coupled with recent observations of the Earth (e.g., Bartholomew *et al.* 1989) and other planets (Potter and Morgan 1981, Tyler *et al.* 1988, Roush *et al.* 1989, Pollack *et al.* 1990, Lucey *et al.* 1989) in the midinfrared and the planned Thermal Emission Spectrometer scheduled as an instrument to be included on the Mars observer all illustrate the increasing interest in the optical properties of materials in the midinfrared and their direct application to remote sensing observations of other planetary surfaces. As the laboratory and observational data increase they will ultimately be modeled to aid in the understanding of the composition and mineralogy of the surface and atmospheric constituents on these bodies. In order to facilitate such quantitative analyses, knowledge regarding the optical constants (real (n) and imaginary (k) indices of refraction) of a wide variety of pertinent materials is required. Examples of the application of such quantitative analyses to the interpretation of Martian surface and atmospheric constituents, based on the optical constants of minerals, are presented in Aronson and Emslie (1975), Toon *et al.* (1977), and Pollack *et al.* (1990).

Optical constants can be readily derived from polished surfaces of cohesive materials using standard geological thin sectioning and polishing techniques. The midinfrared optical constants of only a few specific silicate minerals are available in the literature [e.g., quartz, Spitzer and Kleinman (1961); muscovite and garnet, Aronson and Strong (1975); serpentine and chlorite, Mooney and Knacke (1985); and montmorillonite, Toon *et al.* (1977)]. Additionally, optical constants have been determined for a number of specific rock types including silicates (e.g., Pollack *et al.* 1973, Aronson and Strong 1975) and limestone (Querry *et al.* 1978). Recently optical constants for palagonite, typically a poorly characterized mineralogical assemblage resulting from the alteration of basaltic glass, were presented for a limited wavelength range (Crisp and Bartholomew 1989). The optical constants of many nonsilicate materials are available [e.g., terrestrial atmospheric aerosols, Toon *et al.* (1976); graphite, Draine (1985),

[1] NASA Ames Research Center associate.

0019-1035/91 $3.00

Twitty and Weinman (1971); organic materials, Khare *et al.* (1984), Twitty and Weinman (1971); low temperature condensates, Irvine and Pollack (1968), Roux *et al.* (1979), Sill *et al.* (1980), Warren (1984, 1986), Masterson and Khanna (1990)].

Due to their physical particle size clays and other materials, such as palagonite, can not be prepared using standard geological preparation techniques. Yet in some cases, such as for Mars, these are the materials of perhaps the greatest interest. Here we present a method for the derivation of the optical constants for these less cohesive materials.

2. DERIVATION OF MATHEMATICAL RELATIONSHIPS

In general, we wish to derive the optical constants, i.e., the real, n, and imaginary, k, indices of refraction, of a material as a function of wavelength from a measurement obtained in the laboratory. One technique commonly employed is dispersion analysis (Pollack *et al.* 1973, Aronson and Strong 1975, Toon *et al.* 1976, Querry *et al.* 1978, Mooney and Knacke 1985) which describes n and k as the contributions due to a sum of classical oscillators and relates them via Fresnel's equations for nonnormal incidence, to the measured near-normal reflectivity. Nonlinear least squares techniques can then be used to minimize the differences between the observed and the calculated reflectivities.

2.1. Dispersion Analysis

In dispersion analysis n and k are described in terms the summation of the contributions due to a set of classical oscillators (Spitzer and Kleinman 1961, Pollack *et al.* 1973, Aronson and Strong 1975, Toon *et al.* 1976, Querry *et al.* 1978, Mooney and Knacke 1985) and are expressed as:

$$n^2 - k^2 = \varepsilon_\infty + \sum_{i=1}^{n} \frac{4\pi\rho_i\lambda^2(\lambda^2 - \lambda_i^2)}{(\lambda^2 - \lambda_i^2)^2 + \Gamma_i^2\lambda^2} \tag{1}$$

and

$$nk = \sum_{i=1}^{n} \frac{2\pi\rho_i\lambda^3\Gamma_i}{(\lambda_i^2 - \lambda^2)^2 + \Gamma_i^2\lambda^2}, \tag{2}$$

where each oscillator is described by its characteristic strength $4\pi\rho_i$, width Γ_i, and wavelength λ_i. The high frequency dielectric constant is ε_∞. Let the right hand side of Eqs. (1) and (2) be represented by A and B, respectively, so $n^2 - k^2 = A$ and $k^2 = B^2/n^2$. Substituting for k^2 yields $n^2 - B^2/n^2 = A$. Finding the lowest common denominator, rearranging, and combining all terms on the left gives $n^4 - An^2 - B^2 = 0$. Let $z = n^2$ and this becomes $z^2 - Az - B^2 = 0$, which is quadratic in z. Applying the quadratic formula gives $z = (A \pm \sqrt{A^2 + 4B^2})/2$ or simplifying and resubstituting for z gives $n^2 = (A + \sqrt{A^2 + 4B^2})/2$. Hence, $n = \sqrt{(A \pm \sqrt{A^2 + 4B^2})/2}$. Which results in

$$k = \frac{B}{n} = \frac{B}{\sqrt{\dfrac{A + \sqrt{A^2 + 4B^2}}{2}}}. \tag{3}$$

Replacing A and B yields

$$n = \frac{1}{\sqrt{2}}\left\{\varepsilon_\infty + \sum_{i=1}^{n} \frac{4\pi\rho_i\lambda^2(\lambda^2 - \lambda_i^2)}{(\lambda^2 - \lambda_i^2)^2 + \Gamma_i^2\lambda^2} \pm \left[\left(\varepsilon_\infty + \sum_{i=1}^{n} \frac{4\pi\rho_i\lambda^2(\lambda^2 - \lambda_i^2)}{(\lambda^2 - \lambda_i^2)^2 + \Gamma_i^2\lambda^2}\right)^2 + \left(4\sum_{i=1}^{n} \frac{2\pi\rho_i\lambda^3\Gamma_i}{(\lambda^2 - \lambda_i^2)^2 + \Gamma_i^2\lambda^2}\right)^2\right]^{1/2}\right\}^{1/2} \tag{4}$$

and

$$k = \frac{\sum_{i=1}^{n} \dfrac{4\pi\rho_i\lambda^3\Gamma_i}{(\lambda^2 - \lambda_i^2)^2 + \Gamma_i^2\lambda^2}}{2\sqrt{2}}\left\{\varepsilon_\infty + \sum_{i=1}^{n} \frac{4\pi\rho_i\lambda^2(\lambda^2 - \lambda_i^2)}{(\lambda^2 - \lambda_i^2)^2 + \Gamma_i^2\lambda^2} \pm \left[\left(\varepsilon_\infty + \sum_{i=1}^{n} \frac{4\pi\rho_i\lambda^2(\lambda^2 - \lambda_i^2)}{(\lambda^2 - \lambda_i^2)^2 + \Gamma_i^2\lambda^2}\right)^2 + \left(4\sum_{i=1}^{n} \frac{2\pi\rho_i\lambda^3\Gamma_i}{(\lambda^2 - \lambda_i^2)^2 + \Gamma_i^2\lambda^2}\right)^2\right]^{1/2}\right\}^{-1/2}. \tag{5}$$

Thus, n and k are given in terms of the oscillator parameters ρ_i, Γ_i, and λ_i.

2.2. Fresnel Reflectance

Both n and k can be related to the measured reflectivity at normal incidence (R_n) via Fresnel's equation

$$R_n = \frac{(n - 1)^2 + k^2}{(n + 1)^2 + k^2}. \tag{6}$$

For nonnormal incidence, the intensity and polarization of the light reflected and refracted by the surface can be computed from the Fresnel reflection coefficients, $|r_\perp|^2$ and $|r_\parallel|^2$, which represent the reflected intensity of the light resolved perpendicular and parallel to the plane of

the incident radiation, respectively. The total reflected intensity which can be calculated (R_{calc}) is defined by

$$R_{calc} = \frac{1}{2}\{|r_\perp|^2 + |r_\parallel|^2\}. \quad (7)$$

following Hansen and Travis (1974) and defining i to be the angle of the incident light relative to the surface normal, yields

$$|r_\perp|^2 = \frac{(\sin(90 - i) - u)^2 + v^2}{(\sin(90 - i) + u)^2 + v^2} \quad (8)$$

and

$$|r_\parallel|^2 = \frac{[(n^2 - k^2)\sin(90 - i) - u]^2 + (2nk\sin(90 - i) - v)^2}{[(n^2 - k^2)\sin(90 - i) + u]^2 + (2nk\sin(90 - i) + v)^2} \quad (9)$$

where

$$u = \left\{\frac{n^2 - k^2 - \cos^2(90 - i) + [(n^2 - k^2 - \cos^2(90 - i))^2 + 4n^2k^2]^{1/2}}{2}\right\}^{1/2} \quad (10)$$

and

$$v = \left\{\frac{-(n^2 - k^2 - \cos^2(90 - i)) + [(n^2 - k^2 - \cos^2(90 - i))^2 + 4n^2k^2]^{1/2}}{2}\right\}^{1/2}. \quad (11)$$

Hence if the reflectance of a sample can be measured in the laboratory (R_{meas}), nonlinear least squares techniques (Bevington 1969) can be used to derive the optimal values of n and k by minimizing the differences between R_{meas} and R_{calc}. In our analyses we require that: (1) ρ_i, Γ_i, λ_i all to have values greater than zero; (2) λ_i falls within the range of our observations, i.e., 5 μm $\leq \lambda_i \leq$ 25 μm; and (3) the differences between observed and calculated reflectivities are minimized, i.e., that χ^2 is a minimum.

In our fitting procedure we first chose the number of oscillators based upon the number of obvious peaks in the reflectivity spectrum. ε_∞ is estimated from values of the real index of refraction, $\varepsilon_\infty = n_{vis}^2$, measured in the visible for the appropriate minerals (Deer *et al.* 1966). In order to assess the effect of both n_{vis} and the total number of oscillators on our analysis we vary these parameters and use χ^2 to evaluate the best fit.

2.3. Estimate of Associated Errors

Toon *et al.* (1976) provide an excellent discussion on the relative errors associated with derivation of n and k via dispersion analysis. They conclude that $\Delta n/n$ is a few percent due to errors in the measured reflectivity. In respect to k, if $0.01 < k < 1$, i.e., in the strong bands, then comparison of values derived from dispersion analysis and Kramers–Kronig analysis agree to within a few percent (Toon *et al.* 1976).

At frequencies higher than 2000 cm^{-1} (wavelengths < 5 μm) the assumption that Fresnel reflectivity is the dominant source of reflected light becomes increasingly invalid due to the decrease in the imaginary index of refraction which results in an increasing contribution of multiply scattered light. As a result, optical constants were derived for only the 2000–400 cm^{-1} (5–25 μm) region by our analyses here.

In order to provide an estimate of the errors from our analysis procedure optical constants from several resultant fits, which contain the same number of oscillators but various n_{vis}, were averaged together. These errors can be associated with the derived optical constants, as well as, the oscillator parameters and are included in our following presentation.

3. EXPERIMENTAL

3.1. Mineral Samples

This study was initially conceived in order to aid in the interpretation of Martian surface and atmospheric aerosol mineralogy. The interpretation of remotely sensed data often requires a choice from among a number of fundamental variables. From the perspective of interpreting Mars surface mineralogy we believe that a wider range of surface evolution/modification processes would be implicated by structural rather than compositional variability. Hence we chose to pursue this as the main variable in our study.

The minerals included are biased toward samples which represent hydrated and hydroxylated silicates. These include: (1) the Al and Mg end members of the 1 : 1 layer lattice silicates, kaolinite and serpentine, respectively; (2) an Al-bearing 2 : 1 layer lattice silicate, pyrophyllite; (3) the Mg and Al smectite clays saponite and montmorillonite, respectively; and (4) a palagonite, typically a poorly characterized alteration product of basaltic glass. The kaolinite and montmorillonite clay samples were obtained from the Clay Mineral Society (CMS) and independent chemical analyses and structural characterization are presented by Van Olphen and Fripiat (1979). The saponite, also a CMS sample, has been chemically and structurally characterized by Post (1984). The serpentine was kindly provided by Dr. James Gooding and is a serpentinite from San Luis Obispo, California. Based on its X-ray diffraction (XRD) pattern and differential thermal analysis this sample appears to be ≥95% by weight serpentine (J.

TABLE I
Chemical Analyses of Samples

Sample	SiO_2	Al_2O_3	TiO_2	Fe_2O_3	FeO	MnO	MgO	CaO	Na_2O	K_2O	P_2O_5	LOI^a	$Total$	$Pressure^b$
Kaolinite	44.1	39.3	1.66	0.17	≤0.01	0.02	0.11	0.07	0.07	0.10	0.06	14.8	100.6	3.72
Serpentine														
This Study	38.2	1.11	0.04	4.68	3.7	0.12	37.2	0.64	0.04	0.01	0.02	14.5	100.6	6.89
Mooney & Knacke	40.2	1.31	0.06	c	3.26	0.03	40.1	0.02	≤0.02	≤0.02	n.a.	15.1	100.0	n.a.
Pyrophyllite	n.a.	n.a.	n.a.	n.a.	n.a.	n.a.	n.a.	n.a.	n.a.	n.a.	n.a.	n.a.	n.a.	6.89
Montmorillonite														
This Study	55.0	17.2	0.15	3.62	≤0.01	0.02	2.42	1.21	1.41	0.54	0.05	16.9	98.6	6.89
Toon *et al.*														
219B	63.2	20.6	0.21	3.98	d	0.00	2.14	1.01	2.23	0.26	0.01	5.67	99.31	n.a.
222B	53.1	20.2	0.91	9.90	d	0.21	1.21	0.84	0.18	1.16	0.13	11.9	99.8	n.a.
Saponite[e]	49.6	4.42	0.77	0.80	≤0.01	0.04	22.9	4.18	1.82	1.21	0.11	13.8	99.8	≈0.5
Palagonite	30.7	23.0	4.11	14.6	1.0	0.21	0.87	2.05	0.61	0.47	1.13	21.4	100.4	6.89
Orthopyroxene[f]	55.3	0.12	0.05	c	9.38	0.15	32.80	0.45	0.00	0.02	0.01	2.00	100.3	6.89

Note. n.a., not available.
[a] Lost on ignition, indicative of volatiles.
[b] Pressure, in kbar, to which the pure pellet was pressed in the KBr die.
[c] As FeO.
[d] As Fe_2O_3.
[e] Analysis from Bruckenthal (1987).
[f] Analysis from Singer (1981).

Gooding, personal communication 1991). The pyrophyllite used here has been characterized by Clark *et al.* (1990) as being "spectrally pure." Based on its X-ray diffraction pattern, the palagonite is a sample of an X-ray amorphous weathering product of basaltic glass collected at several locations on the upper slopes of Mauna Kea on the island of Hawaii (Roush 1987). The palagonite sample was separated from the bulk soil sample by liquid particle suspension in methanol. Subsequent transmission electron microscopy of this sample indicates that it is mostly amorphous as more than 75–80% of the grains sampled did not produce an electron diffraction pattern (Roush and Blake 1991). The remaining grains which did diffract electrons exhibited patterns which were consistent with smectite clays (Roush and Blake 1991). Chemical analyses for the samples are provided in Table I.

As our research progressed it became obvious we needed to assess the effects of our nonstandard sample preparation (see following section). In order to facilitate our understanding we included an orthopyroxene because, as discussed below, it represents a material which could be prepared using standard thin sectioning and polishing techniques and as a powdered pellet. The pyroxene used here was obtained from Ward's Scientific and is an enstatite from a locale near Bamle, Norway. A chemical analysis from Singer (1981) is also included in Table I.

3.2. Sample Preparation

Most of the silicates included in this study are clays which are not amenable to standard polishing techniques. In order to obtain a suitable sample of these less cohesive materials for the laboratory measurements a standard KBr pellet die was used and a pellet of the pure sample was prepared. The powders were previously separated by dry sieving and roughly 200 mg of the finest grain size fraction (≤38 μm) were placed in the KBr die. The die was placed in a hydraulic press and the pressure increased to a maximum of roughly 0.5 to 7 kbar on the 12-mm die, depending upon the sample (see Table I), and held at that pressure for 5 min. For all clays and the palagonite this produced a pellet with highly reflective surfaces at visible wavelengths (average surface roughness 0.7 ± 0.4 μm). In contrast, the sole pyroxene prepared by this technique exhibited a matte-like surface (surface roughness ≈5 μm). Inspection of this sample, with a binocular microscope, revealed a pellet which had abundant fine grains of pyroxene adhered to it. In order to semiquantitatively assess the variation of derived optical constants as a function of surface roughness a sample of the pyroxene was also prepared by polishing a large slab of pyroxene to produce a mirror-like surface (surface roughness ≤1 μm).

3.3. Laboratory Measurements and Analyses

The reflectivities of all samples were determined by placing them at the focus of a standard near-normal reflectance attachment located in a Nicolet 7199 Fourier transform spectrometer. A schematic diagram illustrating this device is presented in Fig. 1. The Fourier transform of the signal measured from each sample was ratioed to the Fourier transform of the signal obtained from a first

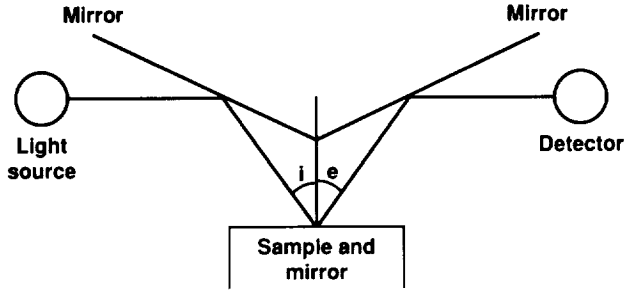

FIG. 1. Schematic diagram of optical path within the spectrometer. For all observations here $i = e = 20°$.

surface aluminum mirror which was conservatively assumed to have a reflectance of 0.96 at all wavelengths. Data were collected from 4000 to 400 cm^{-1} (2.5–25 μm) with a constant spectral resolution of 4 cm^{-1}; however, as discussed above the dispersion analysis was performed only in the 2000–400 cm^{-1} (5.0-25 μm) region. The measured reflectivities of all samples are presented in Figs. 2a, 3a, 4a, 5a, 6a, 7a, and 8a.

Table II lists the final dispersion parameters and associated errors for each sample of this study. We find that the value of n_{vis} for all samples is less than those listed for visible wavelengths (Deer *et al.* 1966). This is due to our analysis covering a finite wavelength region, and the value of n_{vis} listed here is really applicable to the value of n at 5 μm, not visible wavelengths. This is consistent with previous studies of silicates where both visible and infrared optical constants have been derived (e.g., Pollack *et al.* 1973, Mooney and Knacke 1985). The refractive indices (n and k) which provided best comparison to the laboratory reflectance data, as defined by minimizing the sum of the square of the differences between the calculated observed reflectances, were determined. The imaginary indices of refraction (n) are presented for the samples in graph form in Figs. 2b, 3b, 4b, 5b, 6b, 7b, and 8b and are also tabulated in the appendix. The real indices of refraction (k) are presented for the samples in graph form in Figs. 2c, 3c, 4c, 5c, 6c, 7c, and 8c and are also tabulated in the appendix.

4. DISCUSSION

4.1. *Effect of the Physical Nature of the Surface*

As seen in Fig. 2a, the reflectivity of the pyroxene polished slab is roughly three to four times the reflectivity of the pyroxene pure pellet. A comparison of the two surfaces, using a binocular microscope, reveals that the polished slab has a smooth mirror-like surface, whereas the pressed pellet has a rough matte-like surface with obvious fine grains of pyroxene present. We conclude that the polished slab is smooth on the scale of the wavelength, whereas the pellet is rough. The rougher surface results in less Fresnel reflectivity and greater multiply scattered light with the net result being a decrease of the measured reflectance due to the distinctly different physical nature of the two surfaces.

Comparison of the derived oscillator parameters for the

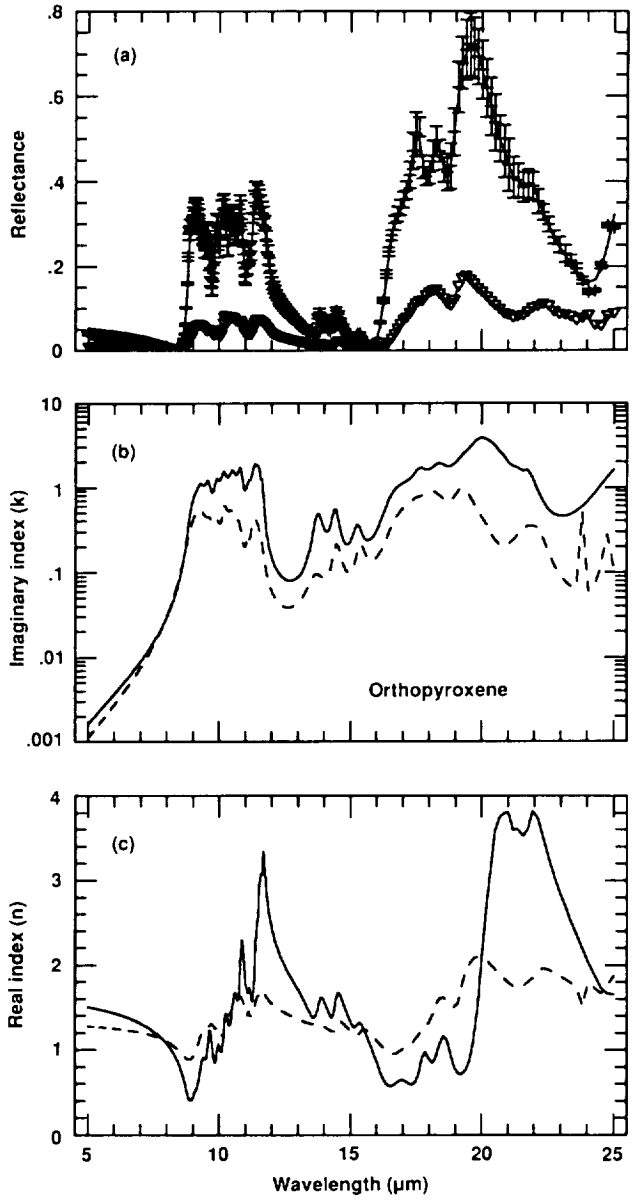

FIG. 2. Measured reflectance of orthopyroxene samples (a). Data points (+) with error bars represent an average of two measurements of the polished slab and the solid line the calculated fit to these data. Triangles (▽) represent the measured reflectance of the pressed pellet and the dashed line a calculated fit to these data. Derived imaginary (b) and real (c) indices of refraction of orthopyroxenes. The solid and dashed line represent the values derived for the polished slab and powdered pellet, respectively.

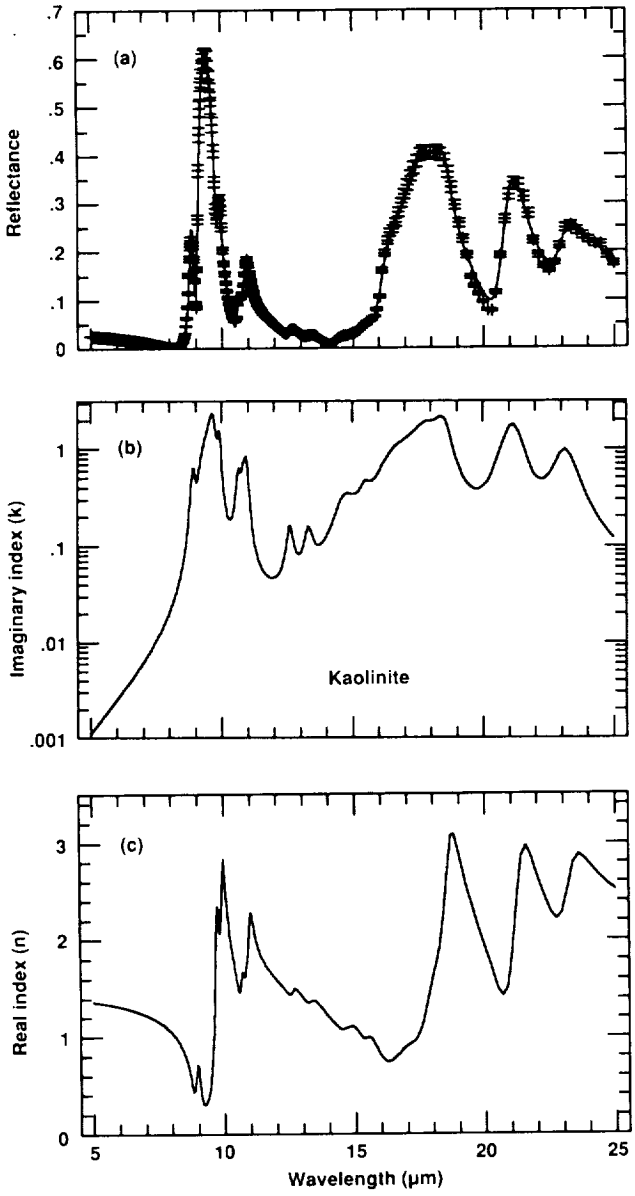

FIG. 3. Measured (points with error bars) and calculated (solid line) reflectances of kaolinite (a). Imaginary (b) and real (c) indices of refraction derived for kaolinite.

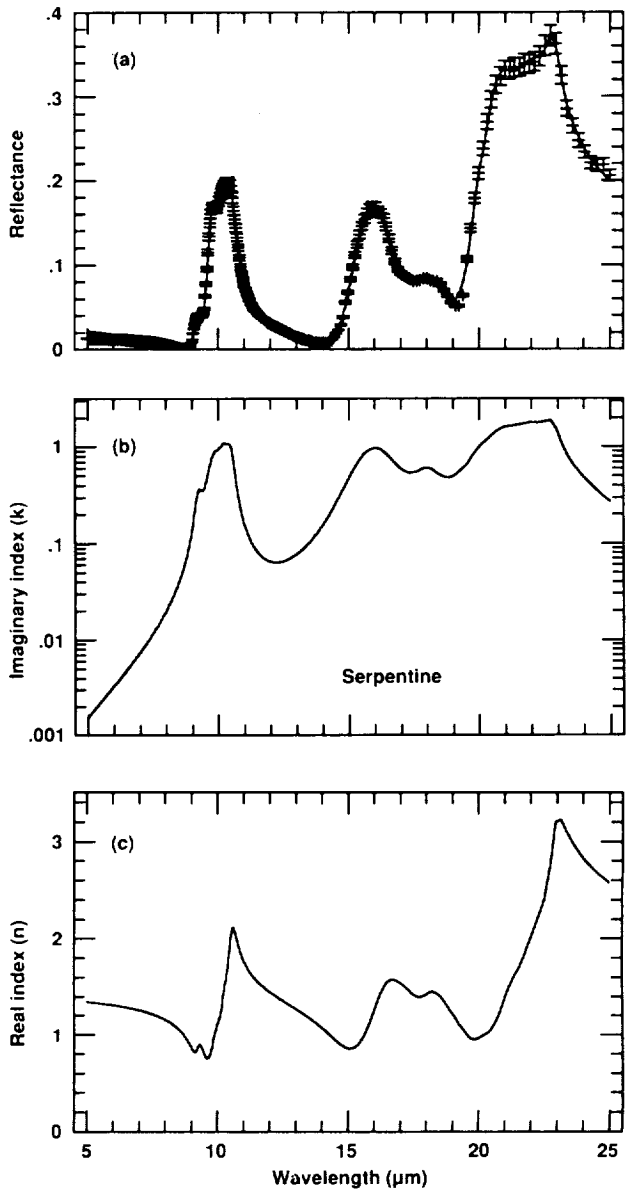

FIG. 4. Measured (points with error bars) and calculated (solid line) reflectances of serpentine (a). Imaginary (b) and real (c) indices of refraction derived for serpentine.

powder and the slab given in Table II immediately shows that one additional oscillator was required to fit the data for the powder. Also n_{vis} derived for the powder is much less than for the slab. The slab n_{vis} is slightly less than, but consistent with, values listed in the visible (Deer *et al.*1966). In general, central wavelengths are shorter, widths are broader, and strengths are less when oscillator parameters for the powder are compared to those of the slab. Figures 2b and 2c illustrate the difference between the derived optical constants of these pyroxene samples. The actual values are tabulated as a function of wavelength in the appendix. In general, the slab k is a factor of 2 to 4 greater than that derived from the powdered pellet, and occasionally in the more intense features greater by a factor of 10. In general, the derived n of both samples agree to within a factor of 2, but again occasionally deviate by slightly more than 2. These results imply that pellets which have a matte finish are not suited for derivation of the optical constants of the materials, and in order to arrive at the closest estimate of n and k, a sample with a mirror-like surface is required.

In contrast to the pyroxene, the pressed pellets of all

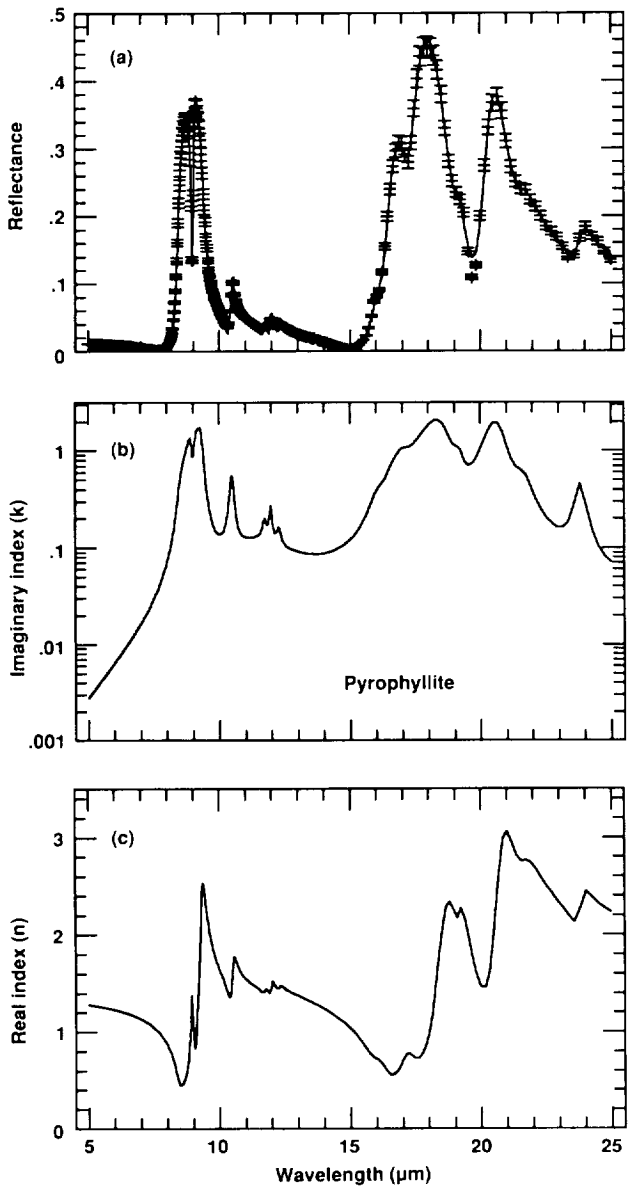

FIG. 5. Measured (points with error bars) and calculated (solid line) reflectances of pyrophyllite (a). Imaginary (b) and real (c) indices of refraction derived for pyrophyllite.

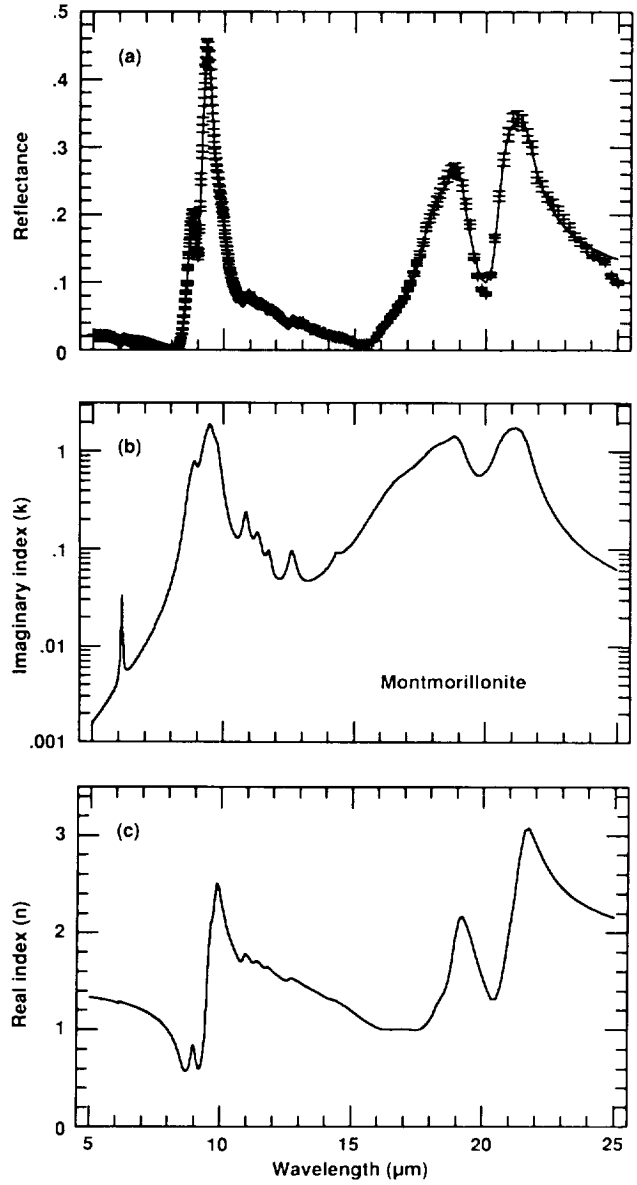

FIG. 6. Measured (points with error bars) and calculated (solid line) reflectances of montmorillonite (a). Imaginary (b) and real (c) indices of refraction derived for montmorillonite.

the other samples exhibited mirror-like surfaces similar to the polished slab of orthopyroxene. Hence, we feel that the values derived and presented here represent a close estimate to the optical constants of these materials. This is especially true at those frequencies (wavelengths) where $k \geq 10^{-2}$.

4.2. Optical Constants in the Region of Adsorbed Water Absorption

Due to extensive isomorphous substitution within their crystalline structure smectite clays readily accommodate exchangeable water molecules between basal tetrahedral layers. As such one would expect the spectral signature of such water to be similar to free molecules, and in transmission and diffuse reflectance spectra of smectites absorptions near 6 μm are observed (e.g., Salisbury *et al.*1987). In the current study we were able to distinguish a distinctive reflectivity peak near 6 μm for both smectites and the palagonite. Although the structural location of the water in palagonite remains uncertain it appears to survive extremes of heating (Bruckenthal 1987). A comparison of the reflectivity of pyrophyllite, a material whose structure

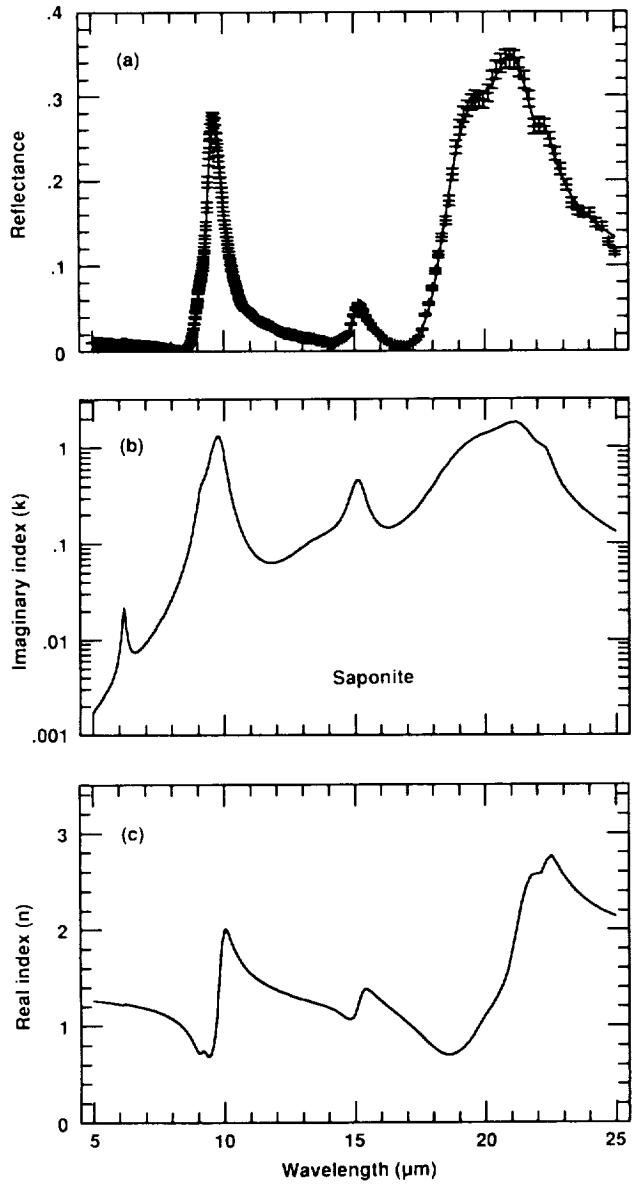

FIG. 7. Measured (points with error bars) and calculated (solid line) reflectances of saponite (a). Imaginary (b) and real (c) indices of refraction derived for saponite.

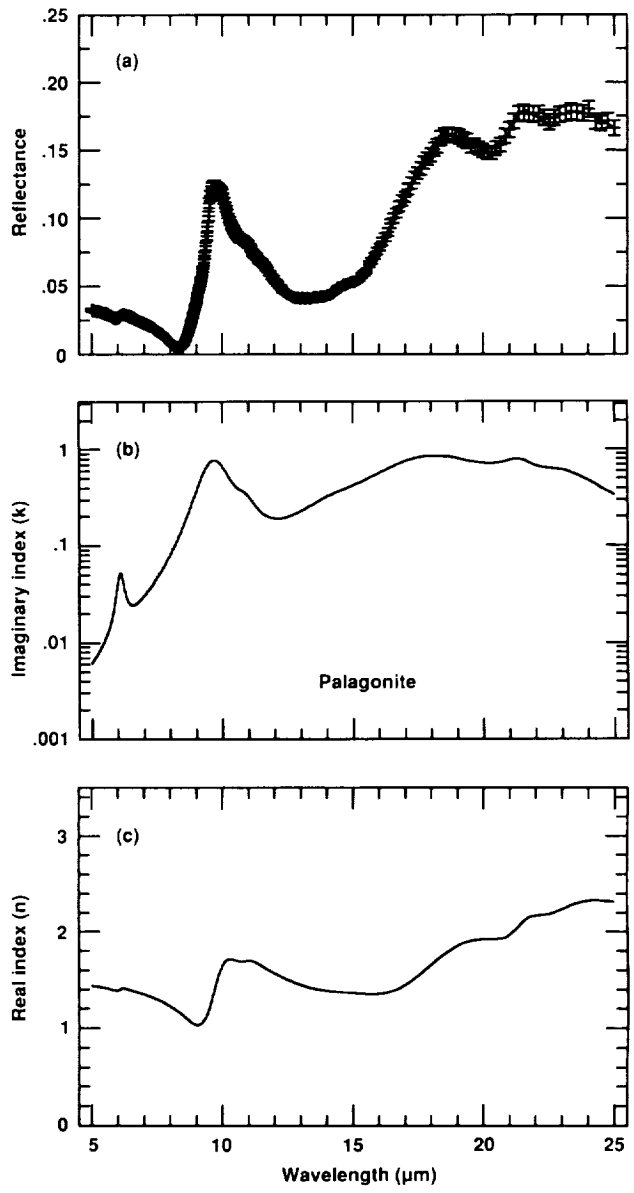

FIG. 8. Measured (points with error bars) and calculated (solid line) reflectances of palagonite (a). Imaginary (b) and real (c) indices of refraction derived for palagonite.

TABLE II
Oscillator Parameters for Silicates

Oscillator	wavelength (μm)	width	strength	Oscillator	wavelength (μm)	width	strength
Orthopyroxene, Slab, n_{vis} = 1.6250±0.0108				12	13.7890±0.0005	0.4261±0.0079	0.0031±0.0000
1	9.0524±0.0077	0.2872±0.0188	0.0006±0.0001	13	14.4380±0.0014	0.3328±0.0009	0.0026±0.0000
2	9.3302±0.0019	0.3531±0.0094	0.0042±0.0002	14	15.2680±0.0010	0.4311±0.0109	0.0014±0.0000
3	9.6021±0.0008	0.2219±0.0018	0.0035±0.0001	15	16.9380±0.0005	1.0319±0.0058	0.0038±0.0001
4	9.9373±0.0004	0.2116±0.0009	0.0025±0.0000	16	17.7750±0.0005	0.4897±0.0018	0.0041±0.0001
5	10.2140±0.0005	0.2528±0.0003	0.0056±0.0001	17	18.4930±0.0009	0.7099±0.0054	0.0093±0.0002
6	10.5370±0.0005	0.3243±0.0004	0.0091±0.0001	18	20.1280±0.0111	0.6864±0.0042	0.0367±0.0038
7	10.8230±0.0005	0.2070±0.0005	0.0084±0.0000	19	20.4970±0.0266	0.5703±0.0271	0.0281±0.0024
8	11.1260±0.0000	0.1925±0.0006	0.0028±0.0000	20	20.8830±0.0324	0.5346±0.0307	0.0164±0.0017
9	11.3820±0.0011	0.2231±0.0015	0.0094±0.0001	21	21.3210±0.0350	0.4748±0.0325	0.0083±0.0011
10	11.6460±0.0004	0.0932±0.0013	0.0029±0.0000	22	21.8080±0.0088	0.6984±0.1219	0.0203±0.0047
11	11.5190±0.0010	0.1590±0.0005	0.0072±0.0001	23	26.6700±0.2729	2.0060±0.1244	0.1264±0.0185

TABLE II—*Continued*

Oscillator	wavelength (μm)	width	strength
Orthopyroxene, Powder, n_{vis} = 1.3200±0.0127			
1	9.0591±0.0250	0.6709±0.1253	0.0022±0.0006
2	9.3089±0.0101	0.5565±0.0324	0.0041±0.0001
3	9.6497±0.0017	0.3538±0.0068	0.0015±0.0001
4	9.9272±0.0013	0.2167±0.0104	0.0007±0.0001
5	10.2290±0.0030	0.2346±0.0022	0.0018±0.0000
6	10.4830±0.0029	0.3737±0.0058	0.0033±0.0001
7	10.7490±0.0048	0.2506±0.0154	0.0012±0.0001
8	11.0800±0.0072	0.0757±0.0446	0.0001±0.0000
9	11.4220±0.0130	0.2796±0.0640	0.0012±0.0002
10	11.3130±0.0189	0.2823±0.0634	0.0012±0.0002
11	11.5750±0.0069	0.2286±0.0262	0.0006±0.0000
12	13.6690±0.0228	0.8135±0.2908	0.0007±0.0002
13	14.4930±0.0033	0.3691±0.0183	0.0009±0.0001
14	15.3960±0.0013	0.4211±0.0208	0.0007±0.0000
15	16.9480±0.0007	1.0682±0.0312	0.0025±0.0002
16	17.5940±0.0008	0.9989±0.0007	0.0038±0.0001
17	18.2740±0.0058	1.0030±0.0046	0.0086±0.0000
18	19.2790±0.0056	0.6767±0.0034	0.0060±0.0000
19	19.5990±0.0130	0.7415±0.0082	0.0031±0.0000
20	19.9660±0.0162	0.9321±0.0363	0.0024±0.0002
21	21.6290±0.0161	1.0250±0.0287	0.0027±0.0002
22	22.1170±0.0112	0.7108±0.0249	0.0019±0.0001
23	23.8240±0.0004	0.0381±0.0094	0.0003±0.0000
24	24.7670±0.0028	0.3594±0.0484	0.0010±0.0001
Kaolinite, n_{vis} = 1.4400±0.0108			
1	8.9326±0.0004	0.1632±0.0009	0.0009±0.0000
2	9.6816±0.0022	0.2193±0.0001	0.0156±0.0006
3	9.9143±0.0024	0.1356±0.0049	0.0067±0.0003
4	10.6350±0.0008	0.1968±0.0041	0.0021±0.0000
5	10.8290±0.0005	0.1877±0.0029	0.0018±0.0000
6	10.9500±0.0013	0.1630±0.0063	0.0032±0.0001
7	12.6050±0.0008	0.2917±0.0026	0.0006±0.0000
8	13.3200±0.0039	0.3668±0.0308	0.0006±0.0001
9	14.7470±0.0138	0.9215±0.0294	0.0024±0.0001
10	15.5010±0.0037	0.4800±0.0024	0.0008±0.0000
11	16.8860±0.0100	1.5651±0.0157	0.0080±0.0005
12	17.9890±0.0075	1.0637±0.0209	0.0197±0.0002
13	18.5560±0.0099	0.5882±0.0084	0.0224±0.0001
14	21.2710±0.0066	0.7674±0.0045	0.0243±0.0000
15	23.2230±0.0028	0.9968±0.0042	0.0155±0.0001
Serpentine, n_{vis} = 1.4000± 0.0158			
1	9.2634±0.0069	0.3302±0.0204	0.0010±0.0001
2	9.8958±0.0032	0.5183±0.0102	0.0045±0.0006
3	10.2480±0.0022	0.4651±0.0270	0.0068±0.0001
4	10.4840±0.0074	0.3175±0.0196	0.0065±0.0004
5	16.2320±0.0187	1.7456±0.0072	0.0209±0.0005
6	18.0870±0.0004	1.1590±0.0185	0.0042±0.0001
7	20.0930±0.0097	0.5377±0.0440	0.0004±0.0001
8	21.0980±0.0230	1.4385±0.0335	0.0095±0.0004
9	22.3150±0.0411	2.2162±0.0640	0.0510±0.0005
10	22.8470±0.0100	0.5532±0.0775	0.0095±0.0004
Pyrophyllite, n_{vis} = 1.3550± 0.0040			
1	8.8448±0.0040	0.1497±0.0041	0.0013±0.0000
2	8.9163±0.0014	0.0698±0.0030	0.0012±0.0001
3	9.1628±0.0005	0.1372±0.0005	0.0021±0.0001
4	9.3058±0.0014	0.2164±0.0027	0.0124±0.0001
5	10.4900±0.0008	0.1761±0.0010	0.0020±0.0000
6	8.7311±0.0054	0.4135±0.0067	0.0020±0.0001
7	11.7240±0.0000	0.1499±0.0025	0.0002±0.0000
8	11.9680±0.0000	0.1199±0.0011	0.0004±0.0000
9	11.2080±0.0826	3.7121±0.1461	0.0077±0.0002
10	12.2850±0.0005	0.1761±0.0141	0.0002±0.0000
11	16.0570±0.0018	0.6447±0.0113	0.0005±0.0000
12	17.0970±0.0005	0.7746±0.0003	0.0029±0.0000
13	18.5260±0.0039	0.9515±0.0014	0.0312±0.0003
14	19.2070±0.0026	0.2852±0.0039	0.0018±0.0000
15	20.7050±0.0029	0.7863±0.0017	0.0286±0.0001
16	21.6820±0.0016	0.7729±0.0235	0.0044±0.0002
17	23.8390±0.0004	0.4701±0.0041	0.0027±0.0000
Saponite, n_{vis} = 1.3134± 0.0028			
1	6.1708±0.0154	0.1916±0.1081	0.0001±0.0001
2	9.1474±0.0002	0.3675±0.0035	0.0008±0.0000
3	9.8531±0.0021	0.4814±0.0017	0.0163±0.0000
4	13.6500±0.0369	3.1476±0.0871	0.0032±0.0000
5	15.1570±0.0014	0.6703±0.0025	0.0033±0.0000
6	20.1070±0.0063	2.3999±0.0092	0.0169±0.0004
7	21.4140±0.0034	1.4703±0.0117	0.0364±0.0003
8	22.3200±0.0036	0.5615±0.0106	0.0040±0.0001
Montmorillonite, n_{vis} = 1.4050± 0.0050			
1	6.1251±0.0004	0.0558±0.0018	0.0001±0.0000
2	8.7293±0.0015	0.3944±0.0078	0.0007±0.0000
3	8.9212±0.0007	0.2563±0.0013	0.0018±0.0000
4	9.5429±0.0011	0.3056±0.0010	0.0136±0.0005
5	9.7748±0.0021	0.3198±0.0082	0.0103±0.0004
6	10.8660±0.0006	0.2866±0.0098	0.0012±0.0001
7	11.3240±0.0015	0.3367±0.0053	0.0007±0.0000
8	11.7390±0.0010	0.1965±0.0066	0.0002±0.0000
9	12.6210±0.0010	0.3401±0.0005	0.0004±0.0000
10	14.3020±0.0053	0.3290±0.0524	0.0001±0.0000
11	16.8460±0.0025	2.4263±0.0281	0.0082±0.0002
12	18.3180±0.0006	1.4641±0.0066	0.0114±0.0001
13	18.9800±0.0030	0.7182±0.0035	0.0118±0.0000
14	20.9160±0.0025	0.8305±0.0012	0.0097±0.0001
15	21.4010±0.0030	0.8047±0.0075	0.0219±0.0002
Palagonite, n_{vis} = 1.5077± 0.0030			
1	6.0961±0.0032	0.3309±0.0148	0.0005±0.0000
2	9.8177±0.0024	1.2525±0.0029	0.0218±0.0001
3	10.9110±0.0015	0.9340±0.0145	0.0025±0.0001
4	14.3460±0.0228	4.0665±0.1040	0.0079±0.0003
5	18.4430±0.0072	5.3360±0.0311	0.0617±0.0003
6	21.4100±0.0095	1.4590±0.0659	0.0058±0.0006
7	23.1830±0.0250	3.4204±0.2421	0.0178±0.0017

does not accommodate exchangeable water, to the reflectivities of the smectites and the palagonite is shown in Fig. 9. Our analyses of these "water-bearing" samples included a single oscillator to describe these features and our results are the first, to our knowledge, to provide optical constants of such materials.

4.3. Comparison to Previous Studies

Montmorillonite. A comparison of our determined optical constants, n and k, of montmorillonite to the tabulated values of two samples of montmorillonite presented by Toon *et al.* (1977) is shown in Figs. 10a and 10b. As seen

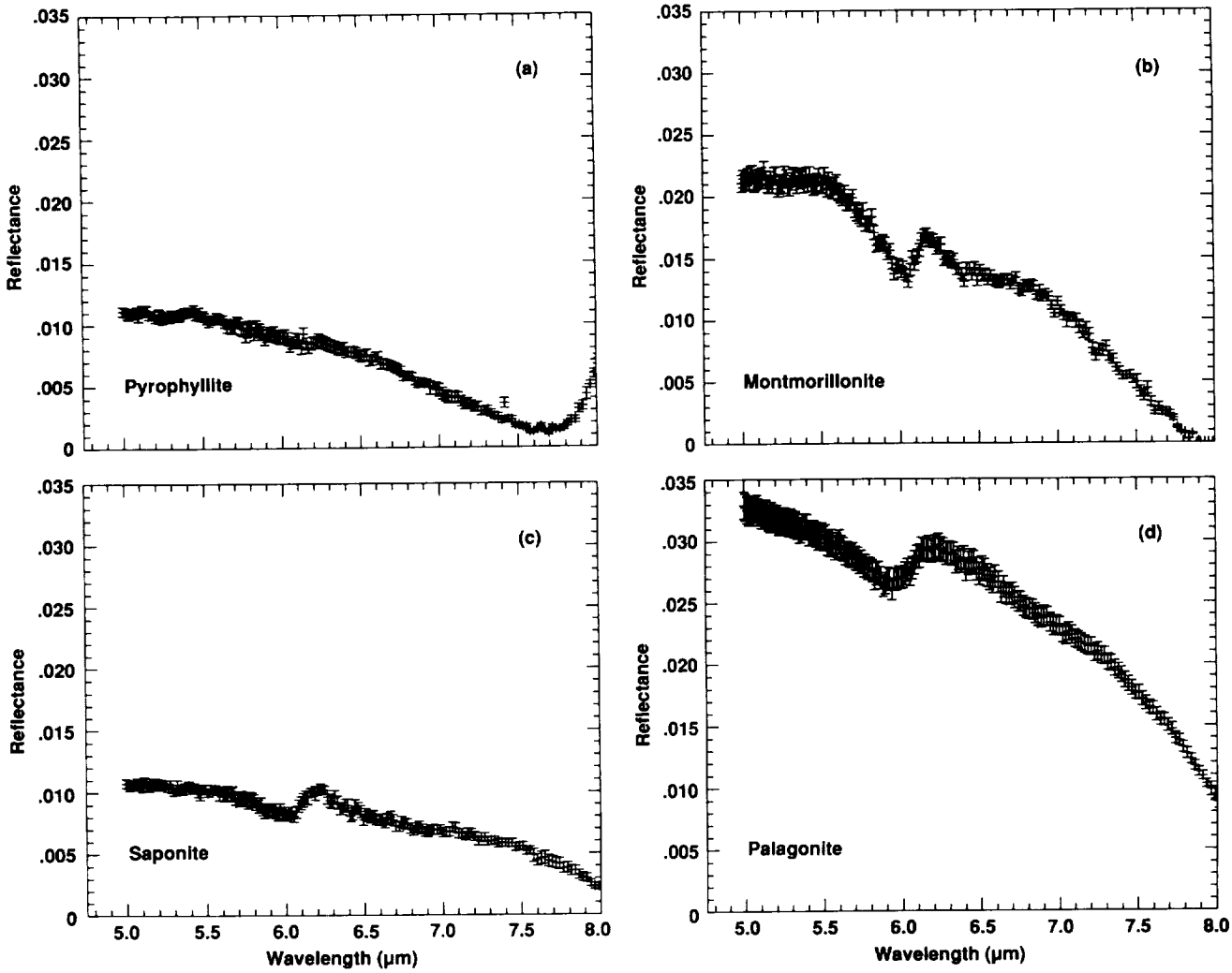

FIG. 9. Measured reflectivities of (a) pyrophyllite, (b) montmorillonite, (c) saponite, and (d) palagonite in the region of adsorbed water absorption.

in these figures the values from the two studies generally agree quite well, although there are some discrepancies. We believe these discrepancies can be explained by differences in sample composition, methods of defining a "best fit" to the reflectivity data, and wavelength coverage of the reflectivity data.

The chemical analyses of the two montmorillonites of Toon *et al.* (1977) are included in Table I. There are obvious differences in the abundances of silicon, iron, magnesium, and sodium between the three samples. As discussed by Farmer (1974) and Russell (1987) the Si–O stretching vibrations near 10 μm are only weakly coupled with other vibrations of the structure of montmorillonites, hence variations of silica content will not strongly influence these features until the structure is significantly altered. On the other hand the Si–O bending vibrations between 17 and 50 μm are strongly coupled with vibrations of the octahedral cations. As a result, the features at 19 and 21 μm can be strongly influenced by iron and magnesium substitution. The octahedral cation–OH bending vibrations occur between 10.5 and 16 μm, thus features in this region will also be strongly affected by compositional differences within the octahedral sites.

Toon *et al.*(1977) derived optical constants from measurements which included the 25- to 40-μm wavelength region. The possibility of additional features at these wavelengths which are not included in the current study is quite real. The existence of any features beyond 400 cm^{-1} (25 μm) would most strongly affect the longest wavelength features observed in the current study. In their analyses Toon *et al.*(1977) estimated when the best comparison between the measured and calculated re-

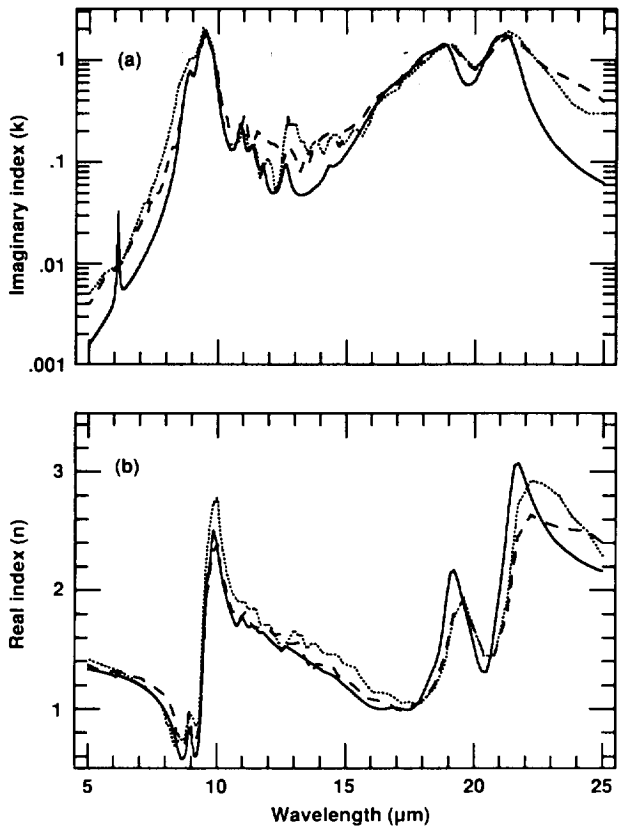

FIG. 10. Comparison of the (a) imaginary and (b) real indices of refraction of montmorillonite derived in this study (solid line) to those previously presented by Toon *et al.*(1977) (dashed line 222B, dotted line 219B).

flectance occurred (O. B. Toon, personal communication 1988) rather than formally minimizing the differences between the two values.

Serpentine. A comparison of our derived values of n and k for serpentine with those of Mooney and Knacke (1985) is presented in Figs. 11a and 11b, respectively. The agreement between the values is generally quite good, although there are some discrepancies. As for the montmorillonite above, we believe these discrepancies can be explained by differences in sample composition, sample preparation, and dispersion analysis techniques. The chemical analysis of the serpentine used by Mooney and Knacke (1985) is included in Table I. There are obvious differences in the abundances of silicon, iron, and magnesium between the two samples. The compositional variation in iron and magnesium would be expected to most strongly affect bands in the 15- to 25-μm wavelength region (Farmer 1974, Russell 1987). If we speculate that some of the ferric iron is substituting for silicon in the tetrahedral layer, then this could explain the apparent shift in the maxima of the real index near 10.5 μm.

The sample of Mooney and Knacke (1985) was a polished slab of serpentine while the current study used a pressed pellet. As discussed above for the orthopyroxene, if the pellet has a matte-like surface the derived values of k will be underestimated and the values of n only approximate. This is in agreement with the differences seen in Fig. 4b. Even though the pellet appeared mirror-like upon inspection with the binocular microscope, we can not rule out the possibility that differences in the physical nature of the two surfaces can explain the discrepencies in the derived optical constants. In their analysis Mooney and Knacke (1985) were able to include data for the 400–200 cm^{-1} (25–50 μm) region while we could not. As discussed above for the montmorillonite, the existence of any features in this region would most strongly affect the longest wavelength features seen in the current study.

Palagonite. Crisp and Bartholomew (1989) presented the imaginary index of refraction of a palagonite in the 1250–500 cm^{-1} (8–20 μm) region for both the hydrated and the dehydrated samples. A comparison of their results with ours is given in Fig. 12. In this case the values we derived for the palagonite generally fall between the two

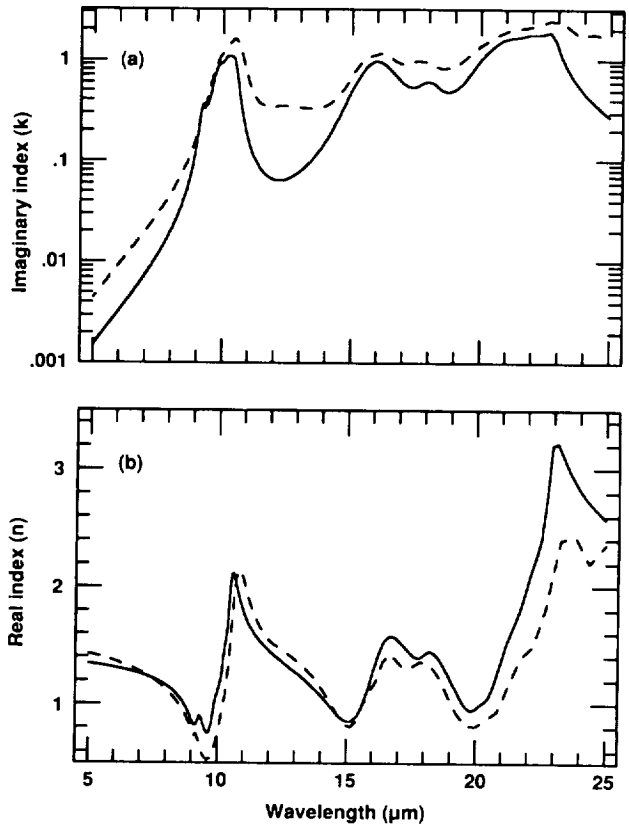

FIG. 11. Comparison of the (a) imaginary and (b) real indices of refraction of serpentine derived in this study (solid line) to those previously presented by Mooney and Knacke (1985) (dashed line).

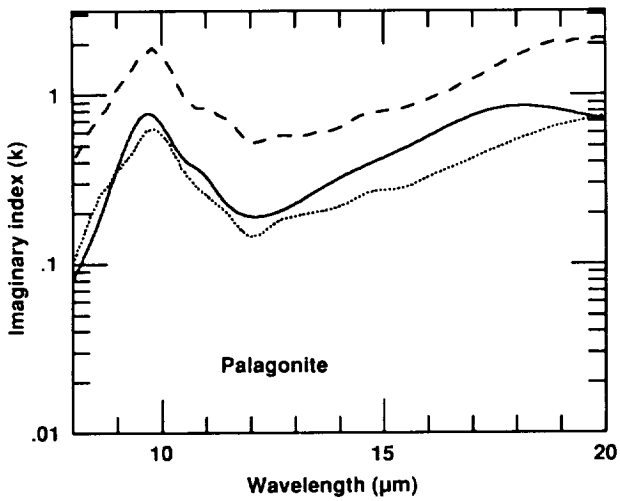

FIG. 12. Comparison of the imaginary index of refraction of palagonite derived in this study (solid line) to those previously presented by Crisp and Bartholomew (1989) for "wet" (dashed line) and "dry" (dotted line) palagonite.

values derived by Crisp and Bartholomew (1989). Some discrepancies still exist, particularly at the longer wavelengths, but this may be due to differences in sample composition, as well as the derivation of values by distinctly different techniques. Crisp and Bartholomew (1989) used transmission measurements, Beer's Law, and assumed the real index of refraction was constant in order to derive the imaginary index of palagonite.

5. CONCLUSIONS

Here we present the real (n) and imaginary (k) indices of refraction of kaolinite, serpentine, montmorillonite, saponite, palagonite, and orthopyroxene as determined by dispersion analysis. We found that comparison of the values derived here for serpentine, montmorillonite, and palagonite to values previously presented were generally consistent. The discrepancies which did exist for these comparisons can be explained by either different sample compositions, sample preparation, or analysis techniques. Comparison of the optical constants derived for both a polished slab and pressed pellet of orthopyroxene led us to conclude that when possible, a polished surface is preferable to a pressed pellet for derivation of optical constants. However, when the physical characteristics of a material preclude preparation of a polished surface the results presented here indicate that if a mirror-like surface is produced, then optical constants can be derived from a pressed pellet of the pure material. Thus, the techniques presented here appear to provide a mechanism for deriving optical constants of clays and other noncohesive materials which may be of interest for interpretation of planetary surface composition.

6. APPENDIX: OPTICAL CONSTANTS

wavelength	Orthopyroxene Slab		Orthopyroxene Powder		Kaolinite		Serpentine		Pyrophyllite		Montmorillonite		Saponite		Palagonite	
(in μm)	n	k	n	k	n	k	n	k	n	k	n	k	n	k	n	k
5.000	1.505	0.002	1.277	0.001	1.362	0.001	1.344	0.002	1.280	0.003	1.336	0.002	1.262	0.002	1.438	0.006
5.010	1.504	0.002	1.277	0.001	1.362	0.001	1.343	0.002	1.280	0.003	1.335	0.002	1.262	0.002	1.438	0.006
5.020	1.503	0.002	1.277	0.001	1.362	0.001	1.343	0.002	1.279	0.003	1.335	0.002	1.262	0.002	1.437	0.006
5.030	1.503	0.002	1.276	0.001	1.361	0.001	1.343	0.002	1.279	0.003	1.335	0.002	1.261	0.002	1.437	0.006
5.040	1.502	0.002	1.276	0.001	1.361	0.001	1.343	0.002	1.278	0.003	1.334	0.002	1.261	0.002	1.436	0.006
5.050	1.502	0.002	1.276	0.001	1.360	0.001	1.342	0.002	1.278	0.003	1.334	0.002	1.261	0.002	1.436	0.006
5.061	1.501	0.002	1.276	0.001	1.360	0.001	1.342	0.002	1.278	0.003	1.333	0.002	1.260	0.002	1.436	0.006
5.071	1.500	0.002	1.276	0.001	1.360	0.001	1.342	0.002	1.277	0.003	1.333	0.002	1.260	0.002	1.435	0.007
5.081	1.500	0.002	1.275	0.001	1.359	0.001	1.341	0.002	1.277	0.003	1.333	0.002	1.260	0.002	1.435	0.007
5.092	1.499	0.002	1.275	0.001	1.359	0.001	1.341	0.002	1.276	0.003	1.332	0.002	1.260	0.002	1.434	0.007
5.102	1.498	0.002	1.275	0.001	1.358	0.001	1.341	0.002	1.276	0.003	1.332	0.002	1.259	0.002	1.434	0.007
5.113	1.498	0.002	1.275	0.001	1.358	0.001	1.340	0.002	1.276	0.003	1.332	0.002	1.259	0.002	1.434	0.007
5.123	1.497	0.002	1.274	0.001	1.357	0.001	1.340	0.002	1.275	0.003	1.331	0.002	1.259	0.002	1.433	0.007
5.134	1.497	0.002	1.274	0.001	1.357	0.001	1.340	0.002	1.275	0.003	1.331	0.002	1.258	0.002	1.433	0.007
5.144	1.496	0.002	1.274	0.001	1.357	0.001	1.340	0.002	1.274	0.003	1.330	0.002	1.258	0.002	1.432	0.007
5.155	1.495	0.002	1.274	0.001	1.356	0.001	1.339	0.002	1.274	0.003	1.330	0.002	1.258	0.002	1.432	0.007
5.165	1.495	0.002	1.273	0.001	1.356	0.001	1.339	0.002	1.273	0.003	1.329	0.002	1.258	0.002	1.431	0.007
5.176	1.494	0.002	1.273	0.001	1.355	0.001	1.339	0.002	1.273	0.003	1.329	0.002	1.257	0.002	1.431	0.007
5.187	1.493	0.002	1.273	0.001	1.355	0.001	1.338	0.002	1.272	0.003	1.329	0.002	1.257	0.002	1.430	0.007
5.198	1.492	0.002	1.273	0.001	1.354	0.001	1.338	0.002	1.272	0.003	1.328	0.002	1.257	0.002	1.430	0.007
5.208	1.492	0.002	1.272	0.001	1.354	0.001	1.338	0.002	1.271	0.003	1.328	0.002	1.256	0.002	1.429	0.007
5.219	1.491	0.002	1.272	0.001	1.353	0.001	1.337	0.002	1.271	0.003	1.327	0.002	1.256	0.002	1.429	0.008
5.230	1.490	0.002	1.272	0.001	1.353	0.001	1.337	0.002	1.270	0.003	1.327	0.002	1.256	0.002	1.429	0.008
5.241	1.490	0.002	1.272	0.001	1.352	0.001	1.337	0.002	1.270	0.003	1.326	0.002	1.255	0.002	1.428	0.008
5.252	1.489	0.002	1.271	0.001	1.352	0.001	1.336	0.002	1.270	0.003	1.326	0.002	1.255	0.002	1.428	0.008
5.263	1.488	0.002	1.271	0.001	1.351	0.001	1.336	0.002	1.269	0.003	1.325	0.002	1.255	0.002	1.427	0.008
5.274	1.487	0.002	1.271	0.001	1.351	0.001	1.336	0.002	1.269	0.003	1.325	0.002	1.254	0.002	1.427	0.008
5.285	1.487	0.002	1.270	0.001	1.350	0.001	1.335	0.002	1.268	0.003	1.324	0.002	1.254	0.002	1.426	0.008
5.297	1.486	0.002	1.270	0.001	1.350	0.001	1.335	0.002	1.268	0.004	1.324	0.002	1.254	0.002	1.426	0.008
5.308	1.485	0.002	1.270	0.001	1.349	0.001	1.335	0.002	1.267	0.004	1.324	0.002	1.253	0.002	1.425	0.008
5.319	1.484	0.002	1.270	0.001	1.349	0.001	1.334	0.002	1.266	0.004	1.323	0.002	1.253	0.002	1.425	0.008

6. APPENDIX—*Continued*

wavelength	Orthopyroxene Slab		Orthopyroxene Powder		Kaolinite		Serpentine		Pyrophyllite		Montmorillonite		Saponite		Palagonite	
(in μm)	n	k	n	k	n	k	n	k	n	k	n	k	n	k	n	k
5.331	1.484	0.002	1.269	0.001	1.348	0.001	1.334	0.002	1.266	0.004	1.322	0.002	1.253	0.002	1.424	0.009
5.342	1.483	0.002	1.269	0.002	1.348	0.001	1.334	0.002	1.265	0.004	1.322	0.002	1.252	0.002	1.423	0.009
5.353	1.482	0.002	1.269	0.002	1.347	0.001	1.333	0.002	1.265	0.004	1.321	0.002	1.252	0.002	1.423	0.009
5.365	1.481	0.002	1.268	0.002	1.347	0.001	1.333	0.002	1.264	0.004	1.321	0.002	1.251	0.002	1.422	0.009
5.376	1.480	0.002	1.268	0.002	1.346	0.001	1.333	0.002	1.264	0.004	1.320	0.002	1.251	0.002	1.422	0.009
5.388	1.480	0.002	1.268	0.002	1.346	0.002	1.332	0.002	1.263	0.004	1.320	0.002	1.251	0.002	1.421	0.009
5.400	1.479	0.002	1.268	0.002	1.345	0.002	1.332	0.002	1.263	0.004	1.319	0.002	1.250	0.003	1.421	0.009
5.411	1.478	0.002	1.267	0.002	1.345	0.002	1.332	0.002	1.262	0.004	1.319	0.002	1.250	0.003	1.420	0.009
5.423	1.477	0.002	1.267	0.002	1.344	0.002	1.331	0.002	1.262	0.004	1.318	0.002	1.250	0.003	1.419	0.010
5.435	1.476	0.002	1.267	0.002	1.343	0.002	1.331	0.002	1.261	0.004	1.318	0.002	1.249	0.003	1.419	0.010
5.447	1.476	0.002	1.266	0.002	1.343	0.002	1.330	0.002	1.260	0.004	1.317	0.002	1.249	0.003	1.418	0.010
5.458	1.475	0.002	1.266	0.002	1.342	0.002	1.330	0.002	1.260	0.004	1.317	0.002	1.248	0.003	1.418	0.010
5.470	1.474	0.002	1.266	0.002	1.342	0.002	1.329	0.002	1.259	0.004	1.316	0.002	1.248	0.003	1.417	0.010
5.483	1.473	0.002	1.265	0.002	1.341	0.002	1.329	0.002	1.259	0.004	1.316	0.002	1.247	0.003	1.416	0.010
5.495	1.472	0.002	1.265	0.002	1.340	0.002	1.329	0.002	1.258	0.004	1.315	0.002	1.247	0.003	1.416	0.010
5.507	1.471	0.002	1.265	0.002	1.340	0.002	1.328	0.002	1.258	0.004	1.314	0.002	1.247	0.003	1.415	0.011
5.519	1.470	0.002	1.265	0.002	1.339	0.002	1.328	0.002	1.257	0.004	1.314	0.002	1.246	0.003	1.414	0.011
5.531	1.469	0.002	1.264	0.002	1.339	0.002	1.327	0.002	1.256	0.004	1.313	0.003	1.246	0.003	1.414	0.011
5.543	1.469	0.003	1.264	0.002	1.338	0.002	1.327	0.002	1.256	0.004	1.313	0.003	1.245	0.003	1.413	0.011
5.556	1.468	0.003	1.263	0.002	1.337	0.002	1.327	0.002	1.255	0.004	1.312	0.003	1.245	0.003	1.412	0.011
5.568	1.467	0.003	1.263	0.002	1.337	0.002	1.326	0.002	1.254	0.004	1.311	0.003	1.245	0.003	1.411	0.012
5.580	1.466	0.003	1.263	0.002	1.336	0.002	1.326	0.002	1.254	0.004	1.311	0.003	1.244	0.003	1.411	0.012
5.593	1.465	0.003	1.262	0.002	1.336	0.002	1.325	0.002	1.253	0.005	1.310	0.003	1.244	0.003	1.410	0.012
5.605	1.464	0.003	1.262	0.002	1.335	0.002	1.325	0.002	1.252	0.005	1.309	0.003	1.243	0.003	1.409	0.012
5.618	1.463	0.003	1.262	0.002	1.334	0.002	1.324	0.002	1.252	0.005	1.309	0.003	1.243	0.003	1.408	0.013
5.631	1.462	0.003	1.261	0.002	1.334	0.002	1.324	0.002	1.251	0.005	1.308	0.003	1.242	0.003	1.408	0.013
5.643	1.461	0.003	1.261	0.002	1.333	0.002	1.324	0.003	1.250	0.005	1.308	0.003	1.242	0.003	1.407	0.013
5.656	1.460	0.003	1.261	0.002	1.332	0.002	1.323	0.003	1.250	0.005	1.307	0.003	1.241	0.003	1.406	0.014
5.669	1.459	0.003	1.260	0.002	1.332	0.002	1.323	0.003	1.249	0.005	1.306	0.003	1.241	0.003	1.405	0.014
5.682	1.458	0.003	1.260	0.002	1.331	0.002	1.322	0.003	1.248	0.005	1.305	0.003	1.240	0.003	1.404	0.014
5.695	1.457	0.003	1.259	0.002	1.330	0.002	1.322	0.003	1.247	0.005	1.305	0.003	1.240	0.004	1.403	0.015
5.708	1.456	0.003	1.259	0.002	1.329	0.002	1.321	0.003	1.247	0.005	1.304	0.003	1.239	0.004	1.403	0.015
5.721	1.455	0.003	1.259	0.002	1.329	0.002	1.321	0.003	1.246	0.005	1.303	0.003	1.238	0.004	1.401	0.016
5.734	1.454	0.003	1.258	0.002	1.328	0.002	1.320	0.003	1.245	0.005	1.302	0.003	1.238	0.004	1.401	0.016
5.747	1.453	0.003	1.258	0.002	1.327	0.002	1.320	0.003	1.245	0.005	1.302	0.003	1.237	0.004	1.400	0.017
5.760	1.452	0.003	1.258	0.002	1.327	0.002	1.319	0.003	1.244	0.005	1.301	0.003	1.237	0.004	1.399	0.017
5.774	1.451	0.003	1.257	0.002	1.326	0.002	1.319	0.003	1.243	0.005	1.300	0.003	1.236	0.004	1.398	0.018
5.787	1.449	0.003	1.257	0.002	1.325	0.002	1.318	0.003	1.242	0.005	1.299	0.003	1.236	0.004	1.397	0.018
5.800	1.448	0.003	1.256	0.002	1.324	0.002	1.318	0.003	1.241	0.005	1.298	0.003	1.235	0.004	1.396	0.019
5.814	1.447	0.003	1.256	0.002	1.324	0.002	1.317	0.003	1.241	0.005	1.298	0.003	1.235	0.004	1.395	0.020
5.827	1.446	0.003	1.255	0.002	1.323	0.002	1.317	0.003	1.240	0.006	1.297	0.003	1.234	0.004	1.393	0.021
5.841	1.445	0.003	1.255	0.002	1.322	0.002	1.316	0.003	1.239	0.006	1.296	0.003	1.233	0.005	1.392	0.022
5.855	1.444	0.003	1.255	0.002	1.321	0.002	1.316	0.003	1.238	0.006	1.295	0.004	1.232	0.005	1.391	0.023
5.869	1.443	0.003	1.254	0.002	1.320	0.002	1.315	0.003	1.237	0.006	1.294	0.004	1.232	0.005	1.390	0.024
5.882	1.441	0.003	1.254	0.002	1.319	0.002	1.315	0.003	1.237	0.006	1.293	0.004	1.231	0.005	1.389	0.025
5.896	1.440	0.003	1.253	0.002	1.319	0.002	1.314	0.003	1.236	0.006	1.292	0.004	1.230	0.005	1.388	0.027
5.910	1.439	0.003	1.253	0.003	1.318	0.002	1.314	0.003	1.235	0.006	1.291	0.004	1.230	0.006	1.387	0.028
5.924	1.438	0.003	1.252	0.003	1.317	0.002	1.313	0.003	1.234	0.006	1.290	0.004	1.229	0.006	1.387	0.030
5.938	1.436	0.003	1.252	0.003	1.316	0.002	1.313	0.003	1.233	0.006	1.289	0.004	1.228	0.006	1.386	0.032
5.952	1.435	0.004	1.251	0.003	1.315	0.002	1.312	0.003	1.232	0.006	1.288	0.004	1.227	0.006	1.385	0.034
5.967	1.434	0.004	1.251	0.003	1.314	0.002	1.311	0.003	1.231	0.006	1.287	0.004	1.227	0.007	1.385	0.036
5.981	1.433	0.004	1.250	0.003	1.314	0.002	1.311	0.003	1.230	0.006	1.285	0.005	1.226	0.007	1.385	0.038
5.995	1.431	0.004	1.250	0.003	1.313	0.002	1.310	0.003	1.229	0.006	1.284	0.005	1.225	0.008	1.385	0.041
6.010	1.430	0.004	1.249	0.003	1.312	0.003	1.309	0.003	1.228	0.006	1.282	0.005	1.224	0.008	1.386	0.043
6.024	1.429	0.004	1.249	0.003	1.311	0.003	1.309	0.003	1.227	0.007	1.281	0.006	1.223	0.009	1.387	0.046
6.039	1.427	0.004	1.248	0.003	1.310	0.003	1.308	0.003	1.226	0.007	1.279	0.007	1.222	0.009	1.388	0.048
6.053	1.426	0.004	1.248	0.003	1.309	0.003	1.308	0.003	1.225	0.007	1.276	0.008	1.221	0.010	1.390	0.050
6.068	1.425	0.004	1.247	0.003	1.308	0.003	1.307	0.003	1.224	0.007	1.274	0.010	1.220	0.011	1.393	0.051
6.083	1.423	0.004	1.247	0.003	1.307	0.003	1.306	0.004	1.223	0.007	1.271	0.013	1.220	0.013	1.395	0.052
6.098	1.422	0.004	1.246	0.003	1.306	0.003	1.306	0.004	1.222	0.007	1.269	0.019	1.219	0.014	1.398	0.053
6.113	1.420	0.004	1.246	0.003	1.305	0.003	1.305	0.004	1.221	0.007	1.272	0.028	1.219	0.016	1.401	0.053
6.128	1.419	0.004	1.245	0.003	1.304	0.003	1.304	0.004	1.220	0.007	1.284	0.033	1.219	0.018	1.403	0.052
6.142	1.417	0.004	1.245	0.003	1.303	0.003	1.304	0.004	1.219	0.007	1.294	0.025	1.221	0.020	1.406	0.050
6.158	1.416	0.004	1.244	0.003	1.302	0.003	1.303	0.004	1.218	0.007	1.294	0.017	1.223	0.022	1.407	0.049
6.173	1.414	0.004	1.243	0.003	1.301	0.003	1.303	0.004	1.217	0.007	1.291	0.012	1.225	0.022	1.409	0.047
6.188	1.413	0.004	1.243	0.003	1.300	0.003	1.302	0.004	1.216	0.008	1.288	0.009	1.227	0.020	1.410	0.045
6.203	1.411	0.004	1.242	0.003	1.299	0.003	1.301	0.004	1.215	0.008	1.286	0.008	1.229	0.019	1.410	0.042
6.219	1.410	0.004	1.242	0.003	1.298	0.003	1.300	0.004	1.213	0.008	1.283	0.007	1.229	0.017	1.410	0.040
6.234	1.408	0.004	1.241	0.003	1.297	0.003	1.300	0.004	1.212	0.008	1.281	0.006	1.229	0.015	1.410	0.038
6.250	1.407	0.005	1.240	0.003	1.296	0.003	1.299	0.004	1.211	0.008	1.280	0.006	1.229	0.014	1.409	0.037
6.266	1.405	0.005	1.240	0.003	1.294	0.003	1.298	0.004	1.210	0.008	1.278	0.006	1.228	0.013	1.408	0.035
6.281	1.403	0.005	1.239	0.004	1.293	0.003	1.298	0.004	1.209	0.008	1.276	0.006	1.227	0.012	1.407	0.033
6.297	1.402	0.005	1.238	0.004	1.292	0.003	1.297	0.004	1.207	0.008	1.275	0.006	1.226	0.011	1.406	0.032
6.313	1.400	0.005	1.238	0.004	1.291	0.003	1.296	0.004	1.206	0.008	1.273	0.006	1.225	0.011	1.405	0.031
6.329	1.398	0.005	1.237	0.004	1.290	0.003	1.295	0.004	1.205	0.009	1.271	0.006	1.224	0.010	1.404	0.030
6.345	1.397	0.005	1.236	0.004	1.288	0.003	1.294	0.004	1.204	0.009	1.270	0.006	1.223	0.010	1.403	0.029
6.361	1.395	0.005	1.236	0.004	1.287	0.003	1.294	0.004	1.202	0.009	1.269	0.006	1.222	0.009	1.401	0.028
6.378	1.393	0.005	1.235	0.004	1.286	0.003	1.293	0.004	1.201	0.009	1.267	0.006	1.221	0.009	1.400	0.027

6. APPENDIX—*Continued*

wavelength	Orthopyroxene Slab		Orthopyroxene Powder		Kaolinite		Serpentine		Pyrophyllite		Montmorillonite		Saponite		Palagonite	
(in μm)	n	k	n	k	n	k	n	k	n	k	n	k	n	k	n	k
6.394	1.391	0.005	1.234	0.004	1.285	0.003	1.292	0.004	1.199	0.009	1.266	0.006	1.220	0.009	1.398	0.027
6.410	1.390	0.005	1.234	0.004	1.283	0.004	1.291	0.005	1.198	0.009	1.264	0.006	1.219	0.008	1.397	0.026
6.427	1.388	0.005	1.233	0.004	1.282	0.004	1.291	0.005	1.197	0.009	1.263	0.006	1.218	0.008	1.395	0.026
6.443	1.386	0.005	1.232	0.004	1.281	0.004	1.290	0.005	1.195	0.009	1.261	0.006	1.217	0.008	1.394	0.025
6.460	1.384	0.005	1.231	0.004	1.279	0.004	1.289	0.005	1.194	0.010	1.260	0.006	1.216	0.008	1.393	0.025
6.477	1.382	0.005	1.231	0.004	1.278	0.004	1.288	0.005	1.192	0.010	1.258	0.006	1.215	0.008	1.391	0.025
6.494	1.380	0.006	1.230	0.004	1.277	0.004	1.287	0.005	1.191	0.010	1.257	0.006	1.214	0.008	1.390	0.025
6.510	1.378	0.006	1.229	0.004	1.275	0.004	1.286	0.005	1.189	0.010	1.256	0.006	1.213	0.007	1.388	0.025
6.527	1.376	0.006	1.228	0.005	1.274	0.004	1.285	0.005	1.188	0.010	1.254	0.006	1.212	0.007	1.387	0.024
6.544	1.374	0.006	1.227	0.005	1.272	0.004	1.284	0.005	1.186	0.010	1.253	0.006	1.211	0.007	1.385	0.024
6.562	1.372	0.006	1.227	0.005	1.271	0.004	1.283	0.005	1.184	0.011	1.251	0.006	1.210	0.007	1.384	0.024
6.579	1.370	0.006	1.226	0.005	1.269	0.004	1.283	0.005	1.183	0.011	1.250	0.007	1.209	0.007	1.382	0.024
6.596	1.368	0.006	1.225	0.005	1.268	0.004	1.282	0.005	1.181	0.011	1.248	0.007	1.208	0.007	1.381	0.024
6.614	1.365	0.006	1.224	0.005	1.266	0.004	1.281	0.005	1.179	0.011	1.246	0.007	1.207	0.007	1.379	0.024
6.631	1.363	0.006	1.223	0.005	1.265	0.004	1.280	0.005	1.177	0.011	1.245	0.007	1.206	0.007	1.378	0.024
6.649	1.361	0.006	1.222	0.005	1.263	0.004	1.279	0.006	1.176	0.011	1.243	0.007	1.204	0.007	1.376	0.025
6.667	1.359	0.006	1.222	0.005	1.262	0.004	1.278	0.006	1.174	0.012	1.241	0.007	1.203	0.007	1.375	0.025
6.685	1.357	0.007	1.221	0.005	1.260	0.005	1.277	0.006	1.172	0.012	1.240	0.007	1.202	0.008	1.373	0.025
6.702	1.354	0.007	1.220	0.005	1.258	0.005	1.276	0.006	1.170	0.012	1.238	0.007	1.201	0.008	1.372	0.025
6.720	1.352	0.007	1.219	0.006	1.256	0.005	1.275	0.006	1.168	0.012	1.236	0.008	1.200	0.008	1.370	0.025
6.739	1.349	0.007	1.218	0.006	1.255	0.005	1.273	0.006	1.166	0.013	1.234	0.008	1.199	0.008	1.369	0.025
6.757	1.347	0.007	1.217	0.006	1.253	0.005	1.272	0.006	1.164	0.013	1.232	0.008	1.197	0.008	1.367	0.026
6.775	1.344	0.007	1.216	0.006	1.251	0.005	1.271	0.006	1.162	0.013	1.231	0.008	1.196	0.008	1.366	0.026
6.793	1.342	0.007	1.215	0.006	1.249	0.005	1.270	0.006	1.160	0.013	1.229	0.008	1.195	0.008	1.364	0.026
6.812	1.339	0.007	1.214	0.006	1.247	0.005	1.269	0.006	1.158	0.013	1.227	0.008	1.194	0.008	1.363	0.026
6.831	1.337	0.008	1.213	0.006	1.245	0.005	1.268	0.006	1.156	0.014	1.225	0.008	1.193	0.008	1.361	0.027
6.849	1.334	0.008	1.212	0.006	1.244	0.005	1.267	0.006	1.153	0.014	1.223	0.009	1.191	0.008	1.359	0.027
6.868	1.331	0.008	1.211	0.006	1.242	0.005	1.266	0.007	1.151	0.014	1.221	0.009	1.190	0.008	1.358	0.027
6.887	1.329	0.008	1.209	0.007	1.240	0.005	1.264	0.007	1.149	0.015	1.219	0.009	1.189	0.008	1.356	0.028
6.906	1.326	0.008	1.208	0.007	1.237	0.006	1.263	0.007	1.146	0.015	1.217	0.009	1.188	0.009	1.355	0.028
6.925	1.323	0.008	1.207	0.007	1.235	0.006	1.262	0.007	1.144	0.015	1.214	0.009	1.186	0.009	1.353	0.028
6.944	1.320	0.008	1.206	0.007	1.233	0.006	1.261	0.007	1.142	0.015	1.212	0.010	1.185	0.009	1.351	0.029
6.964	1.317	0.009	1.205	0.007	1.231	0.006	1.259	0.007	1.139	0.016	1.210	0.010	1.184	0.009	1.349	0.029
6.983	1.314	0.009	1.204	0.007	1.229	0.006	1.258	0.007	1.136	0.016	1.208	0.010	1.182	0.009	1.348	0.030
7.003	1.311	0.009	1.202	0.007	1.227	0.006	1.257	0.007	1.134	0.016	1.205	0.010	1.181	0.009	1.346	0.030
7.023	1.308	0.009	1.201	0.008	1.224	0.006	1.255	0.008	1.131	0.017	1.203	0.010	1.179	0.009	1.344	0.031
7.042	1.305	0.009	1.200	0.008	1.222	0.006	1.254	0.008	1.128	0.017	1.201	0.011	1.178	0.010	1.342	0.031
7.062	1.301	0.009	1.198	0.008	1.220	0.006	1.253	0.008	1.125	0.017	1.198	0.011	1.176	0.010	1.340	0.031
7.082	1.298	0.010	1.197	0.008	1.217	0.007	1.251	0.008	1.122	0.018	1.195	0.011	1.175	0.010	1.339	0.032
7.102	1.295	0.010	1.196	0.008	1.215	0.007	1.250	0.008	1.120	0.018	1.193	0.011	1.173	0.010	1.337	0.033
7.122	1.291	0.010	1.194	0.009	1.212	0.007	1.248	0.008	1.116	0.019	1.190	0.012	1.172	0.010	1.335	0.033
7.143	1.288	0.010	1.193	0.009	1.210	0.007	1.247	0.008	1.113	0.019	1.187	0.012	1.170	0.011	1.333	0.034
7.163	1.284	0.010	1.191	0.009	1.207	0.007	1.245	0.009	1.110	0.020	1.185	0.012	1.168	0.011	1.331	0.034
7.184	1.281	0.011	1.190	0.009	1.204	0.007	1.244	0.009	1.107	0.020	1.182	0.013	1.167	0.011	1.329	0.035
7.205	1.277	0.011	1.188	0.009	1.201	0.008	1.242	0.009	1.103	0.020	1.179	0.013	1.165	0.011	1.327	0.035
7.225	1.273	0.011	1.187	0.010	1.199	0.008	1.240	0.009	1.100	0.021	1.176	0.013	1.163	0.011	1.325	0.036
7.246	1.270	0.011	1.185	0.010	1.196	0.008	1.239	0.009	1.096	0.021	1.173	0.014	1.161	0.012	1.323	0.037
7.267	1.265	0.012	1.183	0.010	1.193	0.008	1.237	0.009	1.092	0.022	1.169	0.014	1.160	0.012	1.321	0.037
7.289	1.262	0.012	1.182	0.011	1.190	0.008	1.235	0.010	1.089	0.023	1.166	0.014	1.158	0.012	1.318	0.038
7.310	1.257	0.012	1.180	0.011	1.187	0.008	1.234	0.010	1.085	0.023	1.163	0.015	1.156	0.012	1.316	0.039
7.331	1.253	0.012	1.178	0.011	1.183	0.009	1.232	0.010	1.081	0.024	1.159	0.015	1.154	0.013	1.314	0.040
7.353	1.249	0.013	1.176	0.011	1.180	0.009	1.230	0.010	1.076	0.024	1.156	0.015	1.152	0.013	1.312	0.041
7.375	1.245	0.013	1.174	0.012	1.177	0.009	1.228	0.010	1.072	0.025	1.152	0.016	1.150	0.013	1.309	0.041
7.396	1.240	0.013	1.173	0.012	1.173	0.009	1.226	0.011	1.068	0.026	1.148	0.016	1.148	0.013	1.307	0.042
7.418	1.235	0.014	1.171	0.012	1.170	0.010	1.224	0.011	1.063	0.027	1.145	0.017	1.146	0.014	1.304	0.043
7.440	1.231	0.014	1.168	0.013	1.166	0.010	1.222	0.011	1.058	0.027	1.141	0.017	1.143	0.014	1.302	0.044
7.463	1.226	0.014	1.166	0.013	1.163	0.010	1.220	0.011	1.053	0.028	1.137	0.018	1.141	0.014	1.299	0.045
7.485	1.221	0.015	1.164	0.014	1.159	0.010	1.218	0.012	1.048	0.029	1.132	0.018	1.139	0.015	1.297	0.046
7.508	1.216	0.015	1.162	0.014	1.155	0.011	1.216	0.012	1.043	0.030	1.128	0.019	1.137	0.015	1.294	0.047
7.530	1.211	0.016	1.160	0.014	1.151	0.011	1.214	0.012	1.038	0.031	1.124	0.020	1.134	0.016	1.292	0.048
7.553	1.205	0.016	1.158	0.015	1.147	0.011	1.212	0.012	1.032	0.032	1.119	0.020	1.132	0.016	1.289	0.049
7.576	1.200	0.017	1.155	0.015	1.142	0.012	1.209	0.013	1.026	0.033	1.114	0.021	1.129	0.016	1.286	0.050
7.599	1.194	0.017	1.153	0.016	1.138	0.012	1.207	0.013	1.020	0.034	1.109	0.022	1.127	0.017	1.283	0.052
7.622	1.189	0.018	1.150	0.016	1.133	0.012	1.205	0.013	1.014	0.035	1.104	0.023	1.124	0.017	1.280	0.053
7.645	1.183	0.018	1.148	0.017	1.129	0.013	1.202	0.014	1.007	0.037	1.099	0.023	1.121	0.018	1.277	0.054
7.669	1.177	0.019	1.145	0.018	1.124	0.013	1.200	0.014	1.000	0.038	1.094	0.024	1.119	0.018	1.274	0.056
7.692	1.170	0.019	1.142	0.018	1.119	0.013	1.197	0.014	0.993	0.039	1.088	0.025	1.116	0.019	1.271	0.057
7.716	1.164	0.020	1.140	0.019	1.114	0.014	1.195	0.015	0.986	0.041	1.082	0.026	1.113	0.019	1.268	0.058
7.740	1.157	0.020	1.137	0.020	1.109	0.014	1.192	0.015	0.978	0.043	1.076	0.027	1.110	0.020	1.265	0.060
7.764	1.151	0.021	1.134	0.020	1.103	0.015	1.189	0.015	0.970	0.045	1.070	0.028	1.107	0.020	1.262	0.062
7.788	1.144	0.022	1.130	0.021	1.098	0.015	1.186	0.016	0.961	0.046	1.063	0.029	1.103	0.021	1.258	0.063
7.813	1.136	0.022	1.127	0.022	1.092	0.016	1.184	0.016	0.952	0.049	1.056	0.031	1.100	0.022	1.255	0.065
7.837	1.129	0.023	1.124	0.023	1.086	0.016	1.181	0.017	0.943	0.051	1.049	0.032	1.097	0.022	1.251	0.067
7.862	1.121	0.024	1.120	0.024	1.080	0.017	1.178	0.017	0.933	0.053	1.042	0.034	1.093	0.023	1.247	0.069
7.886	1.113	0.025	1.117	0.025	1.073	0.018	1.174	0.018	0.923	0.056	1.034	0.035	1.089	0.024	1.244	0.071
7.911	1.105	0.026	1.113	0.026	1.066	0.018	1.171	0.018	0.912	0.059	1.026	0.037	1.086	0.025	1.240	0.073
7.937	1.097	0.027	1.110	0.027	1.059	0.019	1.168	0.019	0.900	0.062	1.018	0.039	1.082	0.026	1.236	0.075
7.962	1.088	0.028	1.105	0.028	1.052	0.020	1.164	0.019	0.888	0.065	1.009	0.041	1.078	0.026	1.232	0.077

6. APPENDIX—*Continued*

wavelength	Orthopyroxene Slab		Orthopyroxene Powder		Kaolinite		Serpentine		Pyrophyllite		Montmorillonite		Saponite		Palagonite	
(in μm)	n	k	n	k	n	k	n	k	n	k	n	k	n	k	n	k
7.987	1.079	0.029	1.101	0.030	1.045	0.021	1.161	0.020	0.875	0.069	1.000	0.043	1.074	0.027	1.228	0.080
8.013	1.069	0.030	1.097	0.031	1.037	0.021	1.157	0.020	0.861	0.074	0.990	0.045	1.069	0.028	1.224	0.082
8.039	1.059	0.032	1.093	0.033	1.029	0.022	1.153	0.021	0.847	0.078	0.980	0.048	1.065	0.029	1.219	0.085
8.064	1.049	0.033	1.088	0.034	1.020	0.023	1.150	0.022	0.831	0.084	0.969	0.050	1.060	0.031	1.215	0.088
8.091	1.038	0.035	1.083	0.036	1.011	0.024	1.146	0.023	0.814	0.090	0.957	0.053	1.055	0.032	1.211	0.091
8.117	1.027	0.036	1.078	0.038	1.002	0.026	1.141	0.023	0.797	0.097	0.945	0.057	1.050	0.033	1.206	0.094
8.143	1.016	0.038	1.073	0.040	0.992	0.027	1.137	0.024	0.777	0.105	0.933	0.061	1.045	0.034	1.201	0.097
8.170	1.004	0.040	1.068	0.042	0.981	0.028	1.133	0.025	0.757	0.114	0.919	0.065	1.040	0.036	1.196	0.100
8.197	0.991	0.042	1.062	0.045	0.971	0.030	1.128	0.026	0.735	0.125	0.905	0.070	1.034	0.037	1.191	0.104
8.224	0.978	0.044	1.056	0.048	0.959	0.031	1.123	0.027	0.711	0.137	0.890	0.075	1.028	0.039	1.186	0.108
8.251	0.964	0.047	1.050	0.050	0.947	0.033	1.118	0.028	0.685	0.152	0.874	0.081	1.022	0.041	1.181	0.112
8.278	0.950	0.050	1.043	0.054	0.934	0.035	1.113	0.029	0.657	0.170	0.856	0.088	1.016	0.043	1.176	0.116
8.306	0.934	0.053	1.037	0.057	0.921	0.038	1.108	0.030	0.627	0.192	0.838	0.096	1.009	0.045	1.170	0.121
8.333	0.918	0.056	1.030	0.061	0.906	0.040	1.102	0.032	0.596	0.218	0.818	0.105	1.002	0.047	1.164	0.125
8.361	0.901	0.060	1.022	0.065	0.891	0.043	1.097	0.033	0.564	0.250	0.797	0.116	0.995	0.050	1.159	0.131
8.389	0.883	0.064	1.014	0.070	0.874	0.046	1.091	0.034	0.532	0.289	0.774	0.129	0.987	0.052	1.153	0.136
8.417	0.864	0.069	1.006	0.076	0.857	0.050	1.084	0.036	0.503	0.336	0.750	0.144	0.979	0.055	1.147	0.142
8.446	0.843	0.074	0.998	0.081	0.837	0.054	1.078	0.038	0.478	0.391	0.725	0.163	0.970	0.058	1.141	0.148
8.475	0.822	0.080	0.989	0.088	0.817	0.059	1.071	0.040	0.459	0.451	0.699	0.185	0.962	0.062	1.135	0.154
8.503	0.798	0.087	0.980	0.095	0.794	0.064	1.064	0.042	0.449	0.516	0.672	0.212	0.952	0.066	1.128	0.161
8.532	0.773	0.095	0.970	0.104	0.770	0.071	1.056	0.044	0.447	0.582	0.645	0.244	0.942	0.070	1.122	0.169
8.562	0.747	0.105	0.961	0.113	0.743	0.079	1.048	0.046	0.453	0.650	0.621	0.282	0.932	0.075	1.115	0.177
8.591	0.718	0.117	0.951	0.124	0.713	0.089	1.040	0.049	0.465	0.716	0.600	0.326	0.920	0.080	1.108	0.185
8.621	0.686	0.130	0.941	0.136	0.680	0.102	1.031	0.052	0.484	0.782	0.585	0.375	0.908	0.086	1.102	0.194
8.651	0.652	0.147	0.930	0.149	0.643	0.119	1.022	0.055	0.507	0.845	0.577	0.426	0.896	0.092	1.095	0.204
8.681	0.616	0.169	0.920	0.165	0.601	0.142	1.012	0.059	0.534	0.907	0.575	0.478	0.883	0.100	1.088	0.214
8.711	0.577	0.195	0.911	0.182	0.555	0.174	1.002	0.063	0.563	0.972	0.579	0.530	0.868	0.108	1.082	0.225
8.741	0.537	0.229	0.902	0.201	0.506	0.220	0.991	0.067	0.598	1.044	0.587	0.582	0.853	0.118	1.075	0.237
8.772	0.496	0.271	0.895	0.223	0.461	0.287	0.979	0.073	0.649	1.126	0.601	0.636	0.837	0.129	1.069	0.250
8.803	0.459	0.324	0.889	0.247	0.433	0.374	0.967	0.079	0.731	1.206	0.625	0.691	0.821	0.143	1.062	0.264
8.834	0.429	0.387	0.886	0.273	0.436	0.475	0.954	0.085	0.839	1.254	0.663	0.742	0.803	0.158	1.056	0.278
8.865	0.410	0.456	0.886	0.300	0.479	0.572	0.940	0.094	0.928	1.288	0.716	0.780	0.785	0.177	1.051	0.294
8.897	0.402	0.528	0.889	0.329	0.567	0.636	0.925	0.103	1.105	1.368	0.777	0.793	0.767	0.198	1.046	0.310
8.929	0.406	0.599	0.896	0.358	0.669	0.628	0.909	0.114	1.377	1.130	0.826	0.774	0.750	0.224	1.041	0.328
8.961	0.420	0.667	0.907	0.386	0.718	0.553	0.892	0.128	1.210	0.866	0.844	0.737	0.734	0.254	1.037	0.347
8.993	0.443	0.728	0.921	0.413	0.685	0.478	0.875	0.144	0.995	0.881	0.824	0.706	0.722	0.288	1.034	0.367
9.025	0.471	0.780	0.939	0.439	0.606	0.448	0.858	0.164	0.868	1.020	0.779	0.697	0.716	0.325	1.033	0.388
9.058	0.497	0.825	0.959	0.462	0.514	0.466	0.841	0.188	0.835	1.212	0.724	0.718	0.716	0.362	1.032	0.410
9.091	0.518	0.868	0.981	0.484	0.431	0.525	0.828	0.218	0.894	1.419	0.671	0.768	0.722	0.397	1.033	0.433
9.124	0.538	0.916	1.007	0.503	0.370	0.611	0.819	0.252	1.055	1.602	0.630	0.841	0.732	0.425	1.035	0.457
9.158	0.566	0.970	1.034	0.520	0.332	0.708	0.819	0.289	1.289	1.683	0.605	0.931	0.741	0.446	1.040	0.482
9.191	0.605	1.026	1.065	0.533	0.312	0.809	0.830	0.325	1.466	1.671	0.598	1.031	0.743	0.463	1.046	0.507
9.225	0.660	1.075	1.099	0.542	0.305	0.911	0.851	0.352	1.610	1.708	0.609	1.139	0.738	0.481	1.054	0.534
9.259	0.728	1.109	1.134	0.544	0.308	1.015	0.875	0.366	1.848	1.752	0.637	1.253	0.726	0.505	1.065	0.560
9.294	0.799	1.120	1.168	0.539	0.320	1.122	0.893	0.366	2.163	1.673	0.684	1.372	0.711	0.538	1.079	0.586
9.328	0.860	1.107	1.198	0.527	0.340	1.233	0.899	0.358	2.423	1.431	0.754	1.494	0.697	0.582	1.095	0.613
9.363	0.896	1.081	1.222	0.510	0.370	1.351	0.891	0.351	2.532	1.121	0.851	1.617	0.687	0.636	1.114	0.638
9.399	0.904	1.059	1.239	0.491	0.411	1.478	0.873	0.351	2.516	0.850	0.982	1.735	0.685	0.698	1.135	0.663
9.434	0.893	1.063	1.248	0.473	0.469	1.615	0.848	0.361	2.441	0.650	1.153	1.836	0.693	0.766	1.160	0.686
9.470	0.887	1.099	1.251	0.460	0.549	1.765	0.821	0.381	2.349	0.509	1.365	1.898	0.711	0.840	1.186	0.707
9.506	0.913	1.161	1.253	0.452	0.662	1.927	0.795	0.412	2.258	0.411	1.601	1.895	0.741	0.916	1.216	0.727
9.542	0.992	1.216	1.256	0.451	0.825	2.099	0.772	0.453	2.175	0.341	1.823	1.815	0.784	0.995	1.248	0.744
9.578	1.114	1.214	1.266	0.451	1.062	2.263	0.756	0.503	2.101	0.290	1.986	1.679	0.842	1.073	1.282	0.757
9.615	1.215	1.124	1.281	0.448	1.397	2.374	0.750	0.560	2.036	0.252	2.078	1.538	0.917	1.149	1.318	0.768
9.653	1.228	0.991	1.299	0.436	1.813	2.342	0.754	0.621	1.978	0.223	2.126	1.432	1.009	1.218	1.355	0.774
9.690	1.155	0.892	1.309	0.414	2.184	2.100	0.771	0.684	1.926	0.201	2.177	1.366	1.122	1.276	1.393	0.777
9.728	1.042	0.861	1.307	0.390	2.350	1.736	0.800	0.744	1.879	0.184	2.259	1.309	1.253	1.315	1.431	0.775
9.766	0.931	0.901	1.293	0.372	2.304	1.436	0.840	0.798	1.837	0.171	2.365	1.221	1.400	1.327	1.468	0.770
9.804	0.857	0.999	1.271	0.367	2.158	1.311	0.889	0.843	1.798	0.160	2.458	1.084	1.553	1.304	1.504	0.760
9.842	0.847	1.125	1.252	0.377	2.065	1.396	0.942	0.876	1.763	0.152	2.504	0.919	1.699	1.243	1.538	0.747
9.881	0.908	1.236	1.249	0.399	2.252	1.582	0.994	0.897	1.730	0.146	2.501	0.759	1.824	1.149	1.570	0.730
9.921	1.013	1.277	1.265	0.409	2.692	1.442	1.040	0.910	1.698	0.142	2.464	0.623	1.917	1.032	1.599	0.711
9.960	1.079	1.237	1.277	0.395	2.840	0.979	1.077	0.920	1.669	0.139	2.409	0.514	1.975	0.908	1.625	0.689
10.000	1.054	1.199	1.260	0.376	2.714	0.640	1.107	0.935	1.640	0.138	2.349	0.430	2.003	0.788	1.647	0.666
10.040	0.994	1.239	1.224	0.378	2.544	0.454	1.135	0.959	1.612	0.138	2.289	0.364	2.006	0.679	1.666	0.641
10.081	0.977	1.348	1.185	0.411	2.393	0.348	1.171	0.992	1.585	0.140	2.232	0.313	1.994	0.584	1.682	0.616
10.121	1.037	1.473	1.166	0.475	2.266	0.284	1.220	1.030	1.557	0.144	2.179	0.272	1.972	0.504	1.694	0.591
10.163	1.173	1.555	1.190	0.557	2.157	0.243	1.285	1.063	1.528	0.150	2.129	0.240	1.944	0.438	1.703	0.566
10.204	1.335	1.539	1.268	0.614	2.062	0.215	1.362	1.082	1.497	0.160	2.084	0.214	1.914	0.382	1.709	0.542
10.246	1.429	1.434	1.360	0.607	1.975	0.198	1.441	1.086	1.464	0.176	2.042	0.193	1.883	0.336	1.713	0.519
10.288	1.413	1.332	1.408	0.561	1.894	0.189	1.514	1.079	1.428	0.202	2.003	0.176	1.853	0.297	1.715	0.498
10.331	1.339	1.310	1.413	0.529	1.817	0.188	1.582	1.075	1.390	0.246	1.966	0.162	1.824	0.265	1.714	0.478
10.373	1.284	1.373	1.414	0.528	1.740	0.195	1.661	1.079	1.359	0.322	1.932	0.151	1.796	0.237	1.713	0.460
10.417	1.295	1.480	1.435	0.542	1.661	0.215	1.769	1.077	1.372	0.442	1.899	0.142	1.770	0.214	1.710	0.444
10.460	1.384	1.574	1.479	0.545	1.580	0.254	1.907	1.033	1.497	0.560	1.868	0.136	1.745	0.194	1.707	0.429
10.504	1.520	1.604	1.526	0.522	1.503	0.325	2.033	0.925	1.694	0.532	1.838	0.132	1.722	0.177	1.702	0.416
10.549	1.639	1.550	1.556	0.481	1.454	0.443	2.105	0.776	1.781	0.390	1.809	0.130	1.700	0.163	1.699	0.406

6. APPENDIX—*Continued*

wavelength	Orthopyroxene Slab		Orthopyroxene Powder		Kaolinite		Serpentine		Pyrophyllite		Montmorillonite		Saponite		Palagonite	
(in μm)	n	k	n	k	n	k	n	k	n	k	n	k	n	k	n	k
10.593	1.679	1.457	1.562	0.441	1.494	0.585	2.118	0.628	1.767	0.278	1.780	0.133	1.679	0.150	1.695	0.396
10.638	1.637	1.407	1.556	0.418	1.617	0.638	2.093	0.506	1.729	0.215	1.752	0.139	1.660	0.139	1.692	0.388
10.684	1.577	1.461	1.558	0.415	1.676	0.586	2.050	0.412	1.691	0.180	1.726	0.152	1.642	0.129	1.690	0.381
10.730	1.608	1.615	1.587	0.409	1.637	0.574	2.003	0.342	1.659	0.160	1.706	0.174	1.625	0.121	1.689	0.375
10.776	1.823	1.752	1.624	0.369	1.615	0.662	1.956	0.289	1.632	0.148	1.698	0.204	1.609	0.113	1.689	0.369
10.823	2.153	1.663	1.630	0.306	1.701	0.761	1.912	0.248	1.609	0.140	1.713	0.234	1.594	0.107	1.690	0.362
10.870	2.305	1.340	1.605	0.252	1.803	0.794	1.872	0.217	1.590	0.136	1.748	0.242	1.579	0.101	1.692	0.354
10.917	2.202	1.054	1.566	0.218	1.954	0.856	1.836	0.191	1.573	0.132	1.777	0.218	1.566	0.096	1.695	0.345
10.965	1.992	0.926	1.520	0.201	2.217	0.748	1.802	0.171	1.558	0.130	1.782	0.183	1.553	0.091	1.697	0.335
11.013	1.782	0.951	1.469	0.204	2.289	0.483	1.771	0.155	1.545	0.129	1.769	0.155	1.540	0.087	1.698	0.324
11.062	1.665	1.101	1.408	0.273	2.218	0.305	1.743	0.141	1.533	0.128	1.749	0.136	1.528	0.084	1.698	0.311
11.111	1.711	1.234	1.462	0.240	2.131	0.210	1.718	0.129	1.522	0.128	1.727	0.128	1.517	0.080	1.697	0.299
11.161	1.742	1.220	1.416	0.253	2.056	0.157	1.694	0.119	1.511	0.128	1.707	0.128	1.506	0.078	1.693	0.286
11.211	1.629	1.268	1.391	0.303	1.994	0.124	1.672	0.111	1.501	0.128	1.692	0.135	1.495	0.075	1.689	0.274
11.261	1.563	1.506	1.406	0.368	1.942	0.103	1.651	0.104	1.491	0.128	1.688	0.145	1.485	0.073	1.683	0.262
11.312	1.720	1.811	1.461	0.415	1.898	0.089	1.632	0.098	1.482	0.129	1.695	0.150	1.476	0.071	1.676	0.252
11.364	2.084	1.952	1.531	0.426	1.860	0.078	1.613	0.093	1.472	0.129	1.704	0.141	1.466	0.069	1.668	0.242
11.416	2.380	1.853	1.598	0.406	1.827	0.071	1.596	0.088	1.462	0.131	1.705	0.123	1.457	0.068	1.660	0.233
11.468	2.559	1.824	1.644	0.360	1.796	0.065	1.580	0.084	1.451	0.133	1.697	0.106	1.448	0.067	1.652	0.226
11.521	2.955	1.701	1.666	0.315	1.769	0.060	1.564	0.080	1.439	0.136	1.682	0.093	1.439	0.066	1.643	0.219
11.574	3.058	1.280	1.689	0.273	1.744	0.056	1.550	0.077	1.425	0.143	1.665	0.086	1.431	0.065	1.634	0.213
11.628	3.071	1.262	1.698	0.213	1.720	0.053	1.535	0.075	1.411	0.158	1.648	0.086	1.423	0.064	1.625	0.208
11.682	3.348	0.784	1.681	0.160	1.698	0.051	1.522	0.073	1.408	0.189	1.637	0.093	1.415	0.064	1.616	0.204
11.737	3.097	0.429	1.653	0.123	1.677	0.050	1.508	0.071	1.442	0.202	1.642	0.099	1.407	0.063	1.607	0.200
11.792	2.882	0.297	1.626	0.100	1.657	0.048	1.495	0.069	1.447	0.176	1.648	0.086	1.400	0.063	1.598	0.197
11.848	2.725	0.231	1.601	0.084	1.637	0.048	1.483	0.068	1.422	0.172	1.639	0.070	1.392	0.063	1.589	0.195
11.905	2.603	0.190	1.579	0.073	1.619	0.047	1.471	0.066	1.397	0.209	1.624	0.060	1.385	0.064	1.581	0.193
11.962	2.503	0.163	1.559	0.065	1.600	0.047	1.459	0.066	1.459	0.276	1.610	0.054	1.378	0.064	1.572	0.192
12.019	2.419	0.143	1.542	0.058	1.582	0.048	1.447	0.065	1.527	0.201	1.596	0.051	1.370	0.065	1.564	0.191
12.077	2.347	0.128	1.526	0.054	1.563	0.049	1.436	0.064	1.500	0.153	1.583	0.050	1.363	0.065	1.555	0.190
12.136	2.282	0.117	1.511	0.050	1.545	0.051	1.425	0.064	1.472	0.141	1.570	0.049	1.357	0.066	1.547	0.190
12.195	2.225	0.108	1.498	0.047	1.526	0.054	1.414	0.064	1.452	0.147	1.558	0.050	1.350	0.067	1.539	0.191
12.255	2.172	0.101	1.485	0.045	1.506	0.058	1.403	0.064	1.451	0.165	1.546	0.051	1.343	0.068	1.531	0.191
12.315	2.124	0.095	1.473	0.043	1.486	0.065	1.392	0.064	1.475	0.159	1.533	0.054	1.336	0.070	1.523	0.192
12.376	2.078	0.091	1.461	0.041	1.465	0.076	1.381	0.064	1.475	0.132	1.521	0.059	1.330	0.071	1.515	0.194
12.438	2.036	0.087	1.451	0.040	1.446	0.095	1.370	0.065	1.461	0.117	1.510	0.067	1.324	0.073	1.507	0.196
12.500	1.995	0.084	1.440	0.039	1.435	0.124	1.359	0.066	1.448	0.109	1.503	0.078	1.317	0.074	1.500	0.198
12.563	1.956	0.082	1.430	0.039	1.447	0.156	1.348	0.067	1.436	0.105	1.505	0.092	1.311	0.076	1.492	0.201
12.626	1.919	0.081	1.420	0.039	1.481	0.160	1.337	0.068	1.425	0.102	1.517	0.097	1.305	0.078	1.485	0.204
12.690	1.882	0.081	1.410	0.039	1.497	0.134	1.327	0.069	1.415	0.100	1.527	0.089	1.299	0.081	1.478	0.207
12.755	1.847	0.081	1.400	0.039	1.487	0.107	1.315	0.070	1.406	0.098	1.526	0.075	1.293	0.083	1.471	0.211
12.821	1.811	0.082	1.391	0.040	1.467	0.091	1.304	0.072	1.397	0.096	1.518	0.064	1.287	0.086	1.464	0.215
12.887	1.776	0.083	1.381	0.041	1.443	0.084	1.293	0.074	1.388	0.095	1.507	0.057	1.282	0.088	1.457	0.219
12.953	1.740	0.086	1.371	0.043	1.419	0.083	1.281	0.076	1.380	0.093	1.495	0.052	1.276	0.091	1.451	0.224
13.021	1.703	0.090	1.362	0.045	1.396	0.087	1.270	0.079	1.371	0.092	1.484	0.050	1.270	0.094	1.444	0.229
13.089	1.666	0.096	1.352	0.047	1.373	0.098	1.258	0.081	1.362	0.091	1.474	0.048	1.265	0.097	1.439	0.234
13.158	1.626	0.104	1.343	0.051	1.355	0.116	1.245	0.084	1.354	0.090	1.463	0.047	1.260	0.099	1.433	0.240
13.228	1.585	0.116	1.334	0.055	1.347	0.140	1.233	0.088	1.345	0.089	1.453	0.047	1.254	0.102	1.427	0.246
13.298	1.542	0.132	1.325	0.061	1.359	0.159	1.220	0.092	1.336	0.089	1.443	0.047	1.249	0.105	1.422	0.252
13.369	1.496	0.156	1.317	0.067	1.377	0.154	1.206	0.096	1.327	0.088	1.433	0.048	1.244	0.108	1.416	0.259
13.441	1.448	0.191	1.310	0.075	1.377	0.133	1.193	0.100	1.317	0.087	1.423	0.049	1.238	0.111	1.412	0.265
13.514	1.403	0.244	1.306	0.083	1.361	0.116	1.179	0.106	1.308	0.087	1.412	0.050	1.233	0.114	1.407	0.273
13.587	1.374	0.322	1.304	0.091	1.339	0.106	1.164	0.111	1.298	0.087	1.402	0.051	1.227	0.117	1.403	0.280
13.661	1.387	0.419	1.305	0.096	1.314	0.102	1.149	0.118	1.287	0.087	1.392	0.053	1.221	0.120	1.399	0.287
13.736	1.464	0.494	1.306	0.096	1.289	0.103	1.133	0.125	1.277	0.087	1.381	0.055	1.214	0.122	1.395	0.295
13.812	1.567	0.489	1.304	0.094	1.264	0.107	1.117	0.133	1.266	0.087	1.370	0.057	1.207	0.126	1.392	0.303
13.889	1.620	0.417	1.297	0.090	1.239	0.113	1.100	0.142	1.254	0.087	1.359	0.060	1.200	0.129	1.389	0.310
13.966	1.606	0.344	1.286	0.088	1.213	0.122	1.082	0.152	1.243	0.088	1.347	0.064	1.191	0.132	1.386	0.318
14.045	1.553	0.302	1.272	0.089	1.187	0.135	1.064	0.164	1.230	0.088	1.335	0.068	1.182	0.137	1.384	0.326
14.124	1.483	0.298	1.255	0.094	1.161	0.151	1.045	0.177	1.217	0.089	1.323	0.075	1.172	0.142	1.382	0.334
14.205	1.413	0.337	1.236	0.108	1.136	0.171	1.025	0.192	1.204	0.091	1.313	0.083	1.160	0.148	1.379	0.343
14.286	1.375	0.432	1.219	0.133	1.113	0.195	1.005	0.209	1.190	0.092	1.308	0.092	1.147	0.156	1.377	0.351
14.368	1.438	0.553	1.216	0.174	1.093	0.225	0.984	0.229	1.175	0.094	1.304	0.093	1.133	0.167	1.375	0.359
14.451	1.600	0.557	1.252	0.215	1.080	0.258	0.963	0.251	1.159	0.096	1.294	0.091	1.118	0.180	1.374	0.367
14.535	1.679	0.425	1.309	0.207	1.076	0.293	0.942	0.277	1.143	0.098	1.281	0.092	1.101	0.199	1.372	0.375
14.620	1.643	0.308	1.330	0.163	1.081	0.323	0.922	0.307	1.125	0.101	1.266	0.095	1.085	0.225	1.370	0.384
14.706	1.571	0.244	1.317	0.127	1.092	0.343	0.902	0.340	1.107	0.105	1.251	0.100	1.071	0.260	1.368	0.393
14.793	1.495	0.216	1.293	0.108	1.103	0.350	0.885	0.379	1.087	0.109	1.235	0.106	1.066	0.306	1.367	0.402
14.881	1.421	0.212	1.266	0.101	1.105	0.347	0.870	0.422	1.066	0.114	1.219	0.113	1.077	0.363	1.365	0.411
14.970	1.351	0.228	1.239	0.102	1.094	0.341	0.860	0.470	1.043	0.120	1.203	0.122	1.116	0.422	1.363	0.420
15.060	1.293	0.268	1.212	0.112	1.070	0.340	0.855	0.522	1.019	0.127	1.186	0.131	1.187	0.462	1.361	0.431
15.152	1.267	0.329	1.187	0.134	1.037	0.350	0.857	0.577	0.992	0.135	1.169	0.142	1.274	0.460	1.359	0.441
15.244	1.294	0.371	1.174	0.169	1.003	0.375	0.866	0.635	0.963	0.146	1.151	0.155	1.345	0.416	1.357	0.452
15.337	1.326	0.344	1.190	0.208	0.979	0.417	0.884	0.695	0.932	0.159	1.133	0.169	1.380	0.351	1.355	0.464
15.432	1.304	0.289	1.231	0.212	0.980	0.459	0.912	0.753	0.898	0.175	1.115	0.186	1.384	0.291	1.353	0.477
15.528	1.244	0.252	1.245	0.179	0.995	0.472	0.950	0.810	0.861	0.196	1.097	0.204	1.370	0.244	1.352	0.490
15.625	1.170	0.238	1.228	0.151	0.983	0.460	0.998	0.861	0.823	0.224	1.079	0.225	1.348	0.210	1.351	0.505
15.723	1.091	0.240	1.199	0.139	0.938	0.460	1.055	0.906	0.784	0.260	1.062	0.248	1.323	0.187	1.351	0.520

6. APPENDIX—*Continued*

wavelength	Orthopyroxene Slab		Orthopyroxene Powder		Kaolinite		Serpentine		Pyrophyllite		Montmorillonite		Saponite		Palagonite	
(in μm)	n	k	n	k	n	k	n	k	n	k	n	k	n	k	n	k
15.823	1.009	0.256	1.167	0.137	0.882	0.486	1.122	0.941	0.750	0.306	1.046	0.274	1.297	0.170	1.352	0.536
15.924	0.924	0.286	1.134	0.144	0.828	0.535	1.196	0.963	0.726	0.357	1.031	0.303	1.272	0.159	1.353	0.553
16.026	0.836	0.332	1.101	0.157	0.784	0.603	1.273	0.970	0.713	0.402	1.019	0.334	1.248	0.152	1.355	0.571
16.129	0.748	0.398	1.068	0.177	0.755	0.682	1.350	0.960	0.696	0.436	1.009	0.367	1.224	0.148	1.359	0.589
16.234	0.669	0.487	1.035	0.205	0.742	0.768	1.421	0.933	0.662	0.472	1.003	0.401	1.201	0.147	1.363	0.609
16.340	0.611	0.596	1.003	0.241	0.745	0.855	1.482	0.893	0.617	0.527	0.999	0.436	1.177	0.147	1.370	0.629
16.447	0.580	0.715	0.975	0.288	0.760	0.939	1.528	0.843	0.578	0.606	0.999	0.470	1.154	0.149	1.378	0.649
16.556	0.575	0.829	0.956	0.345	0.786	1.016	1.559	0.787	0.557	0.704	1.001	0.503	1.130	0.153	1.387	0.670
16.667	0.590	0.931	0.951	0.408	0.818	1.086	1.574	0.731	0.559	0.810	1.004	0.535	1.106	0.158	1.399	0.691
16.779	0.617	1.012	0.962	0.470	0.851	1.149	1.576	0.678	0.588	0.914	1.007	0.564	1.081	0.166	1.412	0.712
16.892	0.641	1.072	0.985	0.524	0.881	1.207	1.566	0.632	0.643	1.003	1.009	0.594	1.055	0.175	1.428	0.732
17.007	0.645	1.120	1.010	0.566	0.904	1.268	1.547	0.594	0.712	1.061	1.008	0.624	1.028	0.185	1.445	0.752
17.123	0.627	1.178	1.031	0.606	0.924	1.339	1.521	0.565	0.766	1.083	1.004	0.657	1.001	0.199	1.465	0.771
17.241	0.600	1.265	1.052	0.651	0.948	1.428	1.491	0.546	0.776	1.095	0.999	0.696	0.972	0.215	1.487	0.789
17.361	0.589	1.388	1.084	0.703	0.987	1.535	1.460	0.538	0.752	1.139	0.993	0.743	0.941	0.234	1.511	0.805
17.483	0.622	1.537	1.131	0.749	1.054	1.656	1.430	0.541	0.729	1.229	0.992	0.800	0.910	0.257	1.536	0.820
17.606	0.730	1.677	1.184	0.780	1.159	1.779	1.406	0.555	0.730	1.355	0.998	0.866	0.877	0.285	1.563	0.832
17.731	0.904	1.717	1.231	0.801	1.304	1.884	1.394	0.577	0.768	1.503	1.018	0.940	0.844	0.318	1.592	0.842
17.857	0.979	1.622	1.272	0.830	1.476	1.951	1.398	0.599	0.847	1.663	1.055	1.016	0.811	0.357	1.621	0.850
17.986	0.898	1.604	1.329	0.869	1.643	1.976	1.417	0.610	0.977	1.826	1.109	1.088	0.779	0.404	1.651	0.855
18.116	0.847	1.722	1.416	0.896	1.783	1.998	1.439	0.601	1.170	1.975	1.175	1.148	0.750	0.458	1.681	0.857
18.248	0.905	1.867	1.520	0.881	1.938	2.075	1.449	0.572	1.438	2.078	1.247	1.196	0.726	0.520	1.712	0.856
18.382	1.047	1.939	1.597	0.816	2.234	2.179	1.438	0.537	1.765	2.081	1.314	1.240	0.709	0.589	1.741	0.853
18.519	1.166	1.875	1.618	0.738	2.715	2.086	1.407	0.506	2.085	1.936	1.383	1.297	0.700	0.663	1.770	0.847
18.657	1.130	1.762	1.588	0.687	3.071	1.645	1.363	0.487	2.293	1.668	1.486	1.380	0.700	0.741	1.796	0.838
18.797	0.971	1.759	1.534	0.693	3.087	1.161	1.309	0.481	2.343	1.381	1.674	1.451	0.710	0.822	1.821	0.827
18.939	0.817	1.898	1.502	0.773	2.936	0.834	1.250	0.489	2.271	1.171	1.942	1.404	0.730	0.904	1.844	0.814
19.084	0.730	2.121	1.559	0.903	2.757	0.637	1.189	0.512	2.172	1.107	2.143	1.183	0.760	0.985	1.864	0.800
19.231	0.712	2.385	1.739	0.976	2.590	0.519	1.126	0.550	2.274	1.038	2.168	0.921	0.800	1.064	1.881	0.786
19.380	0.759	2.678	1.926	0.906	2.439	0.446	1.065	0.606	2.170	0.781	2.080	0.731	0.849	1.140	1.896	0.771
19.531	0.877	3.001	2.026	0.783	2.300	0.403	1.010	0.680	1.958	0.706	1.954	0.621	0.907	1.211	1.907	0.756
19.685	1.098	3.354	2.077	0.661	2.168	0.383	0.967	0.775	1.762	0.736	1.817	0.572	0.972	1.275	1.915	0.742
19.841	1.484	3.701	2.089	0.548	2.039	0.384	0.945	0.889	1.589	0.852	1.678	0.572	1.041	1.332	1.921	0.730
20.000	2.084	3.904	2.080	0.451	1.908	0.407	0.959	1.008	1.467	1.065	1.538	0.624	1.111	1.383	1.924	0.721
20.161	2.713	3.772	2.054	0.365	1.770	0.462	0.990	1.105	1.457	1.368	1.407	0.739	1.179	1.434	1.925	0.716
20.325	3.128	3.527	2.010	0.293	1.626	0.564	1.013	1.207	1.624	1.707	1.315	0.932	1.249	1.490	1.924	0.715
20.492	3.580	3.208	1.955	0.244	1.493	0.743	1.058	1.328	2.018	1.967	1.314	1.194	1.326	1.558	1.925	0.721
20.661	3.744	2.691	1.899	0.215	1.423	1.023	1.139	1.447	2.579	1.942	1.451	1.468	1.426	1.640	1.928	0.734
20.833	3.794	2.400	1.844	0.204	1.505	1.382	1.252	1.546	2.990	1.558	1.721	1.660	1.566	1.726	1.940	0.754
21.008	3.813	1.982	1.793	0.211	1.820	1.717	1.381	1.612	3.062	1.114	2.019	1.724	1.760	1.792	1.965	0.778
21.186	3.595	1.791	1.753	0.238	2.368	1.818	1.503	1.646	2.955	0.823	2.328	1.751	2.003	1.799	2.009	0.796
21.368	3.612	1.714	1.736	0.283	2.853	1.503	1.608	1.670	2.822	0.683	2.744	1.643	2.257	1.712	2.065	0.796
21.552	3.527	1.574	1.755	0.328	2.973	1.047	1.706	1.703	2.753	0.635	3.046	1.266	2.457	1.535	2.117	0.771
21.739	3.609	1.602	1.794	0.347	2.868	0.732	1.819	1.745	2.764	0.563	3.073	0.864	2.560	1.323	2.151	0.733
21.930	3.826	1.318	1.838	0.357	2.709	0.561	1.955	1.779	2.745	0.431	2.968	0.592	2.576	1.150	2.167	0.696
22.124	3.737	0.922	1.914	0.340	2.551	0.485	2.106	1.793	2.670	0.321	2.843	0.425	2.582	1.069	2.174	0.669
22.321	3.510	0.680	1.961	0.253	2.405	0.478	2.255	1.795	2.583	0.251	2.730	0.321	2.715	0.981	2.179	0.652
22.523	3.279	0.552	1.943	0.173	2.280	0.541	2.418	1.828	2.501	0.206	2.634	0.253	2.772	0.721	2.189	0.641
22.727	3.068	0.487	1.906	0.125	2.210	0.685	2.748	1.882	2.426	0.179	2.554	0.206	2.685	0.528	2.205	0.632
22.936	2.877	0.460	1.868	0.097	2.279	0.885	3.200	1.551	2.355	0.164	2.486	0.172	2.588	0.417	2.227	0.620
23.148	2.699	0.459	1.833	0.080	2.535	0.986	3.221	1.079	2.283	0.163	2.428	0.147	2.504	0.344	2.253	0.603
23.364	2.529	0.480	1.796	0.069	2.798	0.844	3.101	0.817	2.205	0.188	2.379	0.127	2.434	0.293	2.278	0.578
23.585	2.362	0.524	1.747	0.066	2.879	0.601	2.990	0.659	2.134	0.288	2.335	0.112	2.374	0.253	2.301	0.547
23.810	2.196	0.596	1.508	0.507	2.839	0.415	2.897	0.549	2.276	0.461	2.297	0.099	2.322	0.222	2.318	0.511
24.038	2.032	0.704	1.791	0.060	2.765	0.298	2.817	0.467	2.446	0.280	2.263	0.089	2.276	0.197	2.328	0.473
24.272	1.875	0.858	1.727	0.069	2.691	0.224	2.747	0.402	2.385	0.152	2.233	0.081	2.235	0.176	2.332	0.436
24.510	1.743	1.069	1.668	0.122	2.625	0.177	2.684	0.350	2.321	0.105	2.206	0.073	2.199	0.159	2.330	0.400
24.752	1.661	1.337	1.770	0.282	2.569	0.144	2.628	0.307	2.272	0.084	2.181	0.067	2.166	0.144	2.325	0.367
25.000	1.653	1.647	1.875	0.115	2.520	0.121	2.578	0.272	2.234	0.072	2.158	0.062	2.136	0.131	2.316	0.337

ACKNOWLEDGMENTS

We thank Lou Allamandola and Ted Bunch for access to their laboratory equipment, and Xander Tielens and Brian Toon for reviews of the original manuscript. We thank Diana Blaney and an anonomous reviewer for helpful comments on the submitted manuscript. This research was supported in part by NASA Geology and Geophysics Program RTOP 151-01-60-01 and NAGW-2212, and NASA Exobiology Program RTOP 199-70-22-11 and 100-52-52-09.

REFERENCES

ARONSON, J. R., AND A. G. EMSLIE 1975. Composition of the martian dust as derived by infrared spectroscopy from Mariner 9. *J. Geophys. Res.* **80,** 4925–4931.

ARONSON, J. R., AND P. F. STRONG 1975. Optical constants of minerals and rocks. *Appl. Opt.* **14,** 2914–2920.

BARTHOLOMEW, M. J., A. B. KAHLE, AND G. HOOVER 1989. Infrared spectroscopy (2.3–20 μm) for the geological interpretation of remote-

ly-sensed multispectral thermal infrared data. *Int. J. Remote Sensing* **10,** 529–544.

BEVINGTON, P. R. 1969. *Data Reduction and Error Analysis for the Physical Sciences,* McGraw-Hill, New York.

BRUCKENTHAL, E. A. 1987. The dehydration of phyllosilicates and palagonites: Reflectance spectroscopy and differential scanning calorimetry, *Master of Science Thesis,* Univ. of Hawaii.

CLARK, R. N., T. V. V. KING, M. KLEJWA, G. A. SWAYZE, AND N. VERGO 1990. High spectral resolution reflectance spectroscopy of minerals. *J. Geophys. Res.* **95,** 12,653–12,680.

CRISP, J., AND M. J. BARTHOLOMEW 1989. Mid-infrared spectroscopy of palagonite, *Lunar Planet. Sci. XX,* 201–202.

DEER, W. A., R. A. HOWIE, AND J. ZUSSMAN 1966. *An Introduction to the Rock Forming Minerals,* Wiley, New York, New York.

DRAINE, B. T. 1985. Tabulated optical properties of graphite and silicate grains. *Astrophys. J. Suppl. Ser.* **57,** 587–594.

FARMER, V. C. 1974. The layer silicates. In *The Infrared Spectra of Minerals* (V. C. Farmer, Ed.), Mineralogical Society Monograph 4, pp. 331–363. Mineralogical Society, London, England.

HANSEN, J. E., AND L. D. TRAVIS 1974. Light scattering in planetary atmospheres. *Space Sci. Rev.* **16,** 527–610.

IRVINE, W. M., AND J. B. POLLACK 1968. Infrared properties of water and ice spheres. *Icarus* **8,** 324–360.

KHARE, B. N., C. SAGAN, E. T. ARAKAWA, F. SUITS, T. A. CALLCOTT, AND M. W. WILLIAMS 1984. Optical constants of organic tholins produced in a simulated Titanian atmosphere: From soft X-rays to microwave frequencies. *Icarus* **60,** 127–137.

LUCEY, P. G., B. R. HAWKE, AND B. C. BRUNO 1989. Thermal infrared spectroscopy of the Moon. *Bull. Am. Astron. Soc.* **21,** 970.

MASTERSON, C. M., AND R. K. KHANNA 1990. Absorption intensities and complex refractive indicies of crystalline HCN, HC_3N, and C_4N_2 in the infrared region. *Icarus* **83,** 83–92.

MOONEY, T., AND R. F. KNACKE 1985. Optical constants of chlorite and serpentine between 2.5 and 50 μm. *Icarus* **64,** 493–502.

POLLACK, J. B., O. B. TOON, AND B. N. KHARE 1973. Optical properties of some terrestrial rocks and glasses. *Icarus* **19,** 372–389.

POLLACK, J. B., T. ROUSH, F. WITTEBORN, J. BREGMAN, D. WOODEN, C. STOKER, O. B. TOON, D. RANK, B. DALTON, AND R. FREEDMAN 1990. Thermal emission spectra of Mars (5.4–10.5 μm): Evidence for sulfates, carbonates, and hydrates. *J. Geophys. Res.* **95,** 14,595–14,627.

POST, J. L. 1984. Saponite from near Ballarat, California, *Clays Clay Miner.* **32,** 147–153.

POTTER, A. E., AND T. H. MORGAN 1981. Observations of silicate restrahlen bands in lunar infrared spectra, *Proc. Lunar Planet. Sci. Conf. 12th,* 703–713.

QUERRY, M. R., G. OSBORNE, K. LIES, R. JORDON, AND R. M. COVENEY, JR. 1978. Complex refractive index of limestone in the visible and infrared. *Appl. Opt.* **17,** 353–356.

ROUSH, T. L. 1987. Characterization of the spectral reflectance of mafic silicates, hydrated silicates, and hydrated silicate-water ice mixtures in the 0.6 to 4.5 μm wavelength region, and applications to planetary science, *Ph.D. Thesis,* Univ. of Hawaii.

ROUSH, T. L., AND D. BLAKE 1991. Characterization of a Mauna Kea palagonite using transmission electron microscopy. *Lunar Planet. Sci. XXII,* 1139–1140.

ROUSH, T., J. POLLACK, C. STOKER, F. WITTEBORN, J. BREGMAN, D. WOODEN, AND D. RANK 1989. CO_3^{2-} and SO_4^{2-}-bearing anionic complexes detected in martian atmospheric dust. *Lunar Planet. Sci. XX,* 928–929.

ROUX, J. A., B. E. WOOD, A. M. SMITH, AND R. R. PLYLER 1979. *Infrared Optical Properties of Thin CO, NO, CH_4, HCl, H_2O, O_2, N_2, Ar, and Air Cryofilms.* Arnold Engineering Development Center, Tech. Rep. AEDC-TR-79-81; NITS accession number AD-A074913.

RUSSELL, J. D. 1987. Infrared Methods. In *A Handbook of Determinative Methods in Clay Mineralogy* (M. J. Wilson, Ed.), pp. 133–173. Chapman and Hall, New York.

SALISBURY, J. W., L. S. WALTER, AND N. VERGO 1987. *Mid-infrared (2.1–25 μm) Spectra of Minerals.* First ed. USGS Open-File Report 87-263.

SALISBURY, J. W., AND L. S. WALTER 1989. Thermal infrared (2.5–13.5 μm) spectroscopic remote sensing of igneous rock types on particulate planetary surfaces. *J. Geophys. Res.* **94,** 9192–9202.

SILL, G., U. FINK, AND J. R. FERRARO 1980. Absorption coefficients of solid NH_3 from 50 to 7000 cm^{-1}. *J. Opt. Soc. Am.* **70,** 724–739.

SINGER, R. B. 1981. Near-infrared spectral reflectance of mineral mixtures: Systematic combinations of pyroxenes, olivine, and iron oxides, *J. Geophys. Res.* **86,** 7967–7982.

SPITZER, W. G., AND D. A. KLEINMAN 1961. Infrared lattice bands of quartz. *Phys. Rev.* **121,** 1324–1335.

TOON, O. B., J. B. POLLACK, AND B. N. KHARE 1976. The optical constants of several atmospheric aerosol species: Ammonium sulfate, aluminum oxide, and sodium chloride. *J. Geophys. Res.* **81,** 5733–5748.

TOON, O. B., J. B. POLLACK, AND C. SAGAN 1977. Physical properties of the particles composing the martian dust storm of 1971–1972. *Icarus* **30,** 663–696.

TWITTY, J. T. AND J. A. WEINMAN 1971. Radiative properties of carbonaceous aerosols. *J. Appl. Meterol.* **10,** 725–731.

TYLER, A. L., R. W. H. KOZLOWSKI, AND L. A.LEBOFSKY 1988. Determination of rock type on Mercury and the Moon through remote sensing in the thermal infrared. *Geophys. Res. Lett.* **15,** 808–811.

VAN OLPHEN, H., AND J. J. FRIPIAT 1979. *Data Handbook for Clay Materials and other Non-Metallic Minerals,* Pergamon Press, New York, New York.

WALTER, L. S. AND J. W. SALISBURY 1989. Spectral characterization of igneous rocks in the 8- to 12-μm region. *J. Geophys. Res.* **94,** 9203–9213.

WARREN, S. G. 1984. Optical constants of ice from the ultraviolet to the microwave. *Appl.Opt.* **23,** 1206–1225.

WARREN, S. G. 1986. Optical constants of carbon dioxide ice. *Appl. Opt.***25,** 2650–2674.